BADGER

GT BADGER

GEORGIA TECH ROTORCRAFT CENTER OF EXCELENCE

Rotorcraft Center of Excellence

Department of Aerospace Engineering

Georgia Institute of Technology

225 North Avenue, Atlanta, GA 30332

BADGER

In response to the 29TH Annual AHS International Student Design Competition – Undergraduate Category

June 2012

Georgia Institute of Technology

Middle East Technical University

Eliya Wing - Team Leader
Georgia Institute of Technology
Undergraduate Student, ewing3@gatech.edu

Juan Pablo Afman - Chief Engineer
Georgia Institute of Technology
Undergraduate Student, jafman3@gatech.edu

Christopher Cofelice - Undergraduate Student
Georgia Institute of Technology
ccofelice3@gatech.edu

Robert Lee– Undergraduate Student
Georgia Institute of Technology
rlee32@gatech.edu

Michael Avera, - Undergraduate Student
Georgia Institute of Technology
mavera3@gatech.edu

Travis Smith– Undergraduate Student
Georgia Institute of Technology
tsmith64@gatech.edu

Ian Moore – Undergraduate Student
Georgia Institute of Technology
imoore6@gatech.edu

Gökçin Çınar – Undergraduate Student
Middle East Technical University
gokcin.cinar@gmail.com

Michael Burn – Undergraduate Student
Georgia Institute of Technology
mburn3@gatech.edu

Özge Sinem Özçakmak – Undergraduate Student
Middle East Technical University
ozgesinemozcakmak@gmail.com

Peter Johnson – Undergraduate Student
Georgia Institute of Technology
peterjohnson@gatech.edu

Yakut Cansev Küçükosman – Undergraduate Student Middle East Technical University
y.c.kucukosman@gmail.com

Dr. Daniel Schrage – Faculty Advisor
Georgia Institute of Technology
daniel.schrage@ae.gatech.edu

Dr. Ilkay Yavrucuk - Faculty Advisor
Middle East Technical University
yavrucuk@metu.edu.tr

GT Students Received Academic Credit:
Rotorcraft Senior Design – AE 4359

Permission for proposal posting granted.

Acknowledgements

The *BADGER* design team would like to thank those who took the time to assist us in the 2012 Design Competition.

Professors:

Dr. Daniel Schrage -Professor, Department of Aerospace Engineering, Georgia Institute of Technology

Dr. Ilkay Yavrucuk – Professor, Department of Aerospace Engineering, Middle East Technical University

Dr. Marilyn Smith- Professor, Department of Aerospace Engineering, Georgia Institute of Technology

Dr. Lakshmi Sankar- Regents Professor, Department of Aerospace Engineering, Georgia Institute of Technology

Dr. Samer Tawfik - Post Doc, Department of Aerospace Engineering, Georgia Institute of Technology

Fellow Students:

Sylvester Ashok- PhD Candidate, Department of Aerospace Engineering, Georgia Institute of Technology

Apinut Sirirojvisuth- PhD Candidate, Department of Aerospace Engineering, Georgia Institute of Technology

Robert Scott - PhD Candidate, Department of Aerospace Engineering, Georgia Institute of Technology

Ritu Marpu - Graduate Student, Department of Aerospace Engineering, Georgia Institute of Technology

Jaikrishnan Vijayakumar- Graduate Student, Department of Aerospace Engineering, Georgia Institute of Technology

David Miculescu- Undergraduate Student, Department of Aerospace Engineering, Georgia Institute of Technology

Fabian Zender – Graduate Student, Department of Aerospace Engineering, Georgia Institute of Technology

Special Acknowledgments

The Badger design team would like to thank especially Dr. Schrage and Dr. Yavrucuk for their experience, knowledge, contribution and most importantly patience, to the next generation of Rotorcraft Engineers.

Table of Contents

LIST OF FIGURES 8
LIST OF TABLES 10
RFP COMPLIANCE 12
1 INTRODUCTION 12
2 VEHICLE SELECTION AND CONFIGURATION 13
2.1 Mission Requirements 13
2.2 Examination of Different Configurations 15
2.3 Analytical Hierarchy Process and Quality Function Deployment 15
2.4 Configuration Trade-off 19
General Comparison 19
Power Efficiency 19
Synchropter's Maneuverability and Agility Capabilities 20
Forward Flight 21
3 PRELIMINARY SYNCHROPTER SIZING 21
3.1 Weight Sizing 21
3.2 Method 21
3.3 Results 22
4 MAIN ROTOR DESIGN 22
4.1 Blade Radius 22
4.2 Aspect Ratio 23
4.3 Tip speed 24
4.4 Number of Blades and Chord length 24
4.5 Twist Optimization Procedure 25
Approach 25
Results 26
4.6 Airfoil Sections 26
5 HUB DESIGN 26
6 PROPULSION 28
6.1 Engine Sizing 28
One Engine vs Two Engines Trade Study 29
6.2 Auxiliary Propulsion Study 29
Auxiliary Yaw Control 29
Fenestron 30
NOTAR 30
Swiveling Pusher Propeller 31
Intermeshing Main Rotors Only 31

6.3 Auxiliary Forward Propulsion 31
Ducted Fan 32
Propeller 32
6.4 Pusher Propeller Sizing 32
Tip Speed 33
Blade Number 33
Airfoil analysis 34
Chord Length 34
6.5 Horizontal Stabilizer 34
7 TRANSMISSION 35
8 AIRFRAME DESIGN 36
8.1 Material Selection 36
8.2 Fuselage Structure 36
8.3 Landing Gear 37
8.4 CG Travel 37
9 COCKPIT DESIGN 38
9.1 Visibility 38
9.2 Avionics 38
9.3 Pilot Cueing System and Envelope Protection 39
10 FLIGHT CONTROL SYSTEM 39
10.1 Modeling and Simulation 39
10.2 Control Mixing 41
10.3 Controller Design 41
SAS, ACAH, RCAH Control Systems 41
Altitude Hold and Velocity Hold 43
10.4 Trimming 43
10.5 Maneuverability and Agility 44
10.6 Fly-By-Light Architecture 44
11 PERFORMANCE ANALYSIS 44
11.1 Sideward Flight Drag Estimation 44
11.2 Forward Flight Drag Estimation 45
11.3 The GT - BADGER Calculator 45
11.4 Forward Flight Performance 46
12 TRAJECTORY OPTIMIZATION 50
12.1 Method 50
12.2 Results 52
13 SURVIVABILITY & SAFETY 52

13.1 Minimum Equipment 52
13.2 Autorotation 53
13.3 H-V Diagram 53
14 FEASIBILITY 53
14.1 Technology Readiness Level 53
14.1 Life-Cycle Cost Analysis 54
15 FINAL SCORE AND SUMMARY 54
16 DETAILED WEIGHT BREAKDOWN 56
17 REFERENCES 60

LIST OF FIGURES

Figure 1. IPPD Design methodology flow map 13
Figure 2. Illustration of the course to scale on the Hudson River 13
Figure 3. General Parameters associated with each maneuver. 14
Figure 4. Ideal Configuration 17
Figure 5. Configuration Comparison Radar Plot 17
Figure 6. TOPSIS Results 17
Figure 7. Discrepancy in performance of the two rotors in a coaxial prop rotor. 20
Figure 8. FOM vs. Thrust Coefficient for Different Solidities from Experiment and Theory. 20
Figure 9. Component Weight Breakdown Pie Chart 22
Figure 10. Maximum Radius to obtain 7ft of clearance from either pylon 23
Figure 11. Illustration of pylon dimensions given from the RFP 23
Figure 12. 15ft safety clearance around all moving parts, drawn to scale 23
Figure 13. Historical trends of the blade chord lengths as a function of gross weight 23
Figure 14. Range of acceptable tip speeds 24
Figure 15. Drag characteristics of the VR7B airfoil 24
Figure 16. Acceptable chord lengths for tip speeds ranging from 600 to 750 ft/s and aspect ratios from 15 to 20 24
Figure 17. Representative Plot of Optimizing Thrust Margin for a Given Total Linear Twist 26
Figure 18. Optimization Plot Max Thrust Margin with Respect to Linear Twists, whose Maximum Thrust Margins were Found in a Manner as Shown in Figure 12 26
Figure 19. Qualitative hub system assessment 27
Figure 20. Views of the hub spring system from patent (first row) and hub spring on the Badger (bottom row) 27
Figure 21. Servo flap on the Kaman K-Max 28
Figure 22. Load factor capability in forward flight 28
Figure 23. Highlighted portions indicate yawing maneuvers throughout the course 29

Figure 24. Fenestron 30
Figure 25. Aerotécnica AC-14 Directed Jet Thruster with Additional Forward Thrust Ability 30
Figure 26. NOTAR System Diagram 30
Figure 27. Free body diagrams of the Badger in sideward flight 31
Figure 28. Nose Down Angle Required for Steady, Level Flight vs. Airspeed with no Auxiliary Forward Propulsion 31
Figure 29. Forward Flight Behavior Without Auxiliary Propulsion System 32
Figure 30. Forward Flight Behavior with Auxiliary Propulsion System 32
Figure 31. Geometry of final propeller blade selection 33
Figure 32. Effects of blade number on the power required and the blades radius 33
Figure 33. Plot of torque produced by propeller and the counter roll moment produced by the asymmetric wing 35
Figure 34: Illustration of rotor clearance. Not to scale 35
Figure 35. Top view schematic of transmission 35
Figure 36: Badger's airframe with engine, fuel tank, and transmission placement 37
Figure 37. FEA on Landing Gear 37
Figure 38. C.G. Travel throughout Race 37
Figure 39 Marenco Swisshelicoper 38
Figure 40. Badger Visibility with compliance to RFP Requirements 38
Figure 41. Inside View of Cockpit 38
Figure 42. Skyview Display 38
Figure 43. Cargo Hook 39
Figure 44. SIMULINK Non-linear Flight Dynamics Model Constructed from Heli-Dyne+ 40
Figure 45. Controller block diagram 41
Figure 46. Pilot Pitch Input and Augmented Response in Hover using ACAH 42
Figure 47. Pilot Roll Input and Augmented Response in Hover using ACAH 42
Figure 48. Pilot Roll Step Input, Roll Rate and Roll Angle Response using RCAH at 80 knots 42
Figure 49. Pilot Pitch Step Input, Pitch Rate and Pitch Angle Response using RCAH at 80 knots 42
Figure 50. Outer loop (left) and inner loop (right) block diagrams 43
Figure 51 Side Velocity Command Response 43
Figure 52 Forward Velocity Command Response 43
Figure 53. Handling Qualities in the roll axis, (Padfield, 1996) 44
Figure 54. Pressure magnitude color map for fuselage in sideward flight. 44
Figure 55. Velocity Color Map for Fuselage in Sideward Flight 44
Figure 56. Path lines colored by velocity magnitude (m/s). Freestream velocity is in the positive y direction 45
Figure 57. Forward flight drag breakdown 45
Figure 58. GT-Badger Calculator. 46
Figure 59. Plot illustrating how the induced power correction factor is a function of mast separation 46

Figure 60. Induced Power as mast distance grows 46
Figure 61. Power Vs. Velocity (No auxiliary propulsion) 47
Figure 62. Illustrating the 125 kts requirement at 90% MCP 47
Figure 63. A plot showing how the power required is affected by increased gross weight 47
Figure 64. Power Required Curve for both race configurations after addition of a pusher propeller 48
Figure 65. Horsepower v.s. Velocity (knots) with the addition of the pusher propeller meeting requirements given by the RFP 48
Figure 66. Performance contrast of an 80 deg F vs the required 103 deg F 49
Figure 67. Lift to Drag Ratio Vs Velocity in Knots of The BADGER 49
Figure 68. Maximum Rate of Climb (ft/min) Vs. Velocity (knots) 49
Figure 69. Minimum Turn Radius (ft) vs. Velocity (knots) 50
Figure 71. Eigenvalues plotted 50
Figure 70. Competition Course Distance Map 50
Figure 72. Scaled Course Map 51
Figure 73. Course Optimal Trajectory Waypoints 51
Figure 74. Optimal Trajetory 52
Figure 75. Switlik ISPLR 52
Figure 76. Fire Extinguisher 53
Figure 77. BAE S7000 Seat 53
Figure 78. Autorotative Index 53
Figure 79. H-V Diagram 53

LIST OF TABLES

Table 1: Complete list of mission segments. 14
Table 2: Morphological Matrix 15
Table 3: List of Chosen Configurations 15
Table 4: Prioritization Matrix 16
Table 5: Configuration Comparison 16
Table 6: Normalized Configuration Comparison 16
Table 7: Closeness Factors 17
Table 8: Quality Function Deployment 18
Table 9: Advantages and Disadvantages of Intermeshing Configuration 19
Table 10: Configuration Characteristics Based on Momentum Theory. 19
Table 11: Component weight breakdown 22
Table 12: Dimensions of main rotor disk 25
Table 13: Parameters Initialized by Other Considerations 25
Table 14: Baseline Rotor Optimized by Thrust Margin 26

Table 15: Engine Performance 29
Table 16: Fuel Distribution 29
Table 17: One Engine vs. Two Engines 29
Table 18: Morphological matrix of airfoil selection 34
Table 19: JavaProp results of the four airfoil configurations 34
Table 20: Dimensions of final auxiliary propeller 34
Table 21: Dimensions and location of the asymmetric wing 35
Table 22: Gear Sizing 36
Table 23: Minimum Requirements by MIL STD 850B 38
Table 24: Forward Flight Drag Breakdown 45
Table 25: Summary of Figure 65 showing values are in compliance with RFP 48
Table 26: Segment Conditions Table 52
Table 27: Required Equipment 53
Table 28: Breakdown of Development Cost 54

RFP COMPLIANCE

General RFP Requirements		
	Requirement	**Section**
General Design	Pylon Clearance	4.1
	15ft minimum clearance safety zone	4.1
	MIL STD weight breakdown 1374	Appendix
	MIL STD VISIBILITY 850 B	9.1
	Inboard and outboard Profiles of the aircraft	8, 9
	Appropriate weight allocations for all components	8.4
	Preliminary structural design	8.1
	Flotation and fire protection for pilot	12.1
Performance	Fuel Burned throughout mission	6.1
	15 min fuel reserve @ V_BR	3.1
	Slung Load System	11.2
	Accounted power installation factors	2.4, 6.1, 11.3
	HOGE Takeoff	11.3
	HOGE @ S.L. 103° F, TOGW	11.3
	Cruise at a min of 125 kts @ 90 % MCP	11.3
	60 KNOT S.W. flight S.L. 103° F, TOGW	6.2
	Max Start speed < 100 kts	11.2
	Time Estimate	11.2
Operation	Max bank angle of 90°	6.2
	Avionics Suite meeting Min FAA req. for NY VFR corridor	9.2
	5 min requirement to takeoff	9.2
	Special consideration WRT emergency	8.3, 13.1
	Pilot Feedback	10
	10 min. warm up time	9.2
	One 225lb Pilot	3.1
OEC		2, 14

1 INTRODUCTION

The American Helicopter Society's 29th annual student design competition Request for Proposal (RFP), sponsored by Sikorsky and AHS, stipulates the desire for a lightweight, highly maneuverable rotorcraft system. The rotorcraft must be capable of performing at levels similar to the fixed-wing red bull competition aircraft, in order to spark interest in a helicopter racing sport. The designed vehicle will complete an unprecedented collection of maneuvers ranging from slung loaded sideward flight to 360° pirouettes.

The Badger is a single-pilot, highly maneuverable, intermeshing rotorcraft system designed in response to this proposal. The Badger takes its name from the infamous honey badger, a fearless animal who despite its size and misleading figure, is described as the most fearless creature in the entire animal kingdom. The Badger rotorcraft system utilizes an extremely unconventional intermeshing rotor concept, unheard of for maneuverability purposes. The following report, outlines the Badger Team's research and design process, and reinforces the decision to utilize this very unique operating concept. Careful consideration

was taken at each step of the design process in order to strike a balance between fuel efficiency, engine power, load factor, and speed, all while maintaining safety for the pilot and spectators.

2 VEHICLE SELECTION AND CONFIGURATION

The first step in designing the Badger was creating an "Integrated Product/Process Development (IPPD)" methodology. In the conceptual design procedure, the IPPD methodology assists the designers in investigating the requirements set by the RFP and attaining promising solutions. The IPPD works by organizing the very iterative design process in a systematic way. Normal IPPDs contain four loops: the conceptual design loop, initial product data management loop, preliminary design iteration loop, and the process design iteration loop (Schrage).

The process starts with analyzing the requirements set by the RFP and selecting a baseline model. An RF (required fuel) method is then used the size the baseline vehicle. After the vehicle's size was assessed, the even more iterative process of analyzing the individual components began. Several trade studies were completed. Examples of these are basic helicopter configurations, auxiliary propulsion types, main rotor airfoils, hub configuration and transmission selection.

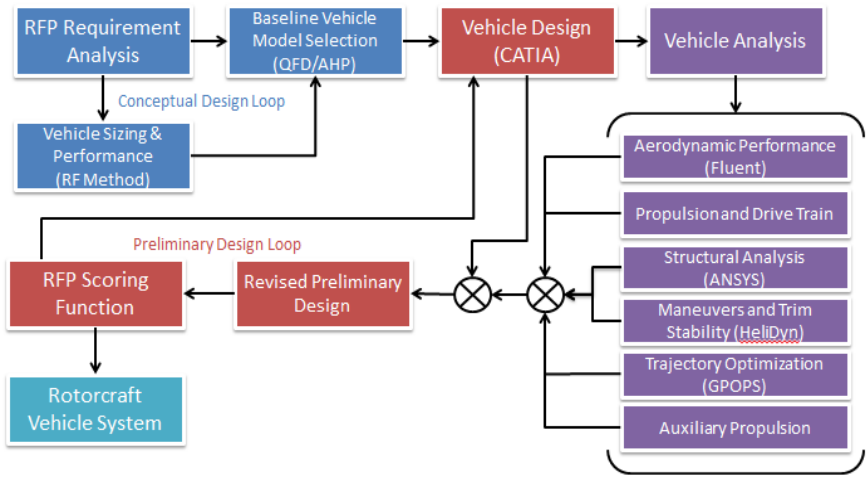

Figure 1. IPPD Design methodology flow map

Once the most ideal solutions were obtained and integrated within the CATIA model, the revised design was scored using the RFP OEC (Overall evaluation criteria) shown below.

$$\eta = 2 * CourseTime[sec] + 5 * Fuel_{consumed}[lbs] + MRP_{S.L,ISA,Uninstalled}[SHP]$$

This process was repeated until the minimal OEC was achieved thereby marking the final helicopter design. The Badger's final score is 1380.6.

2.1 Mission Requirements

According to the RFP, the three most stringent requirements are that the helicopter must be sized to successfully hover at 103°F at Sea Level, achieve a minimum of 60 knots sideward flight, and achieve a minimum of 125 knots at 90% MRP at 103°F at Sea Level. The course, however, is assumed to be flown at 80°F at Sea Level since the race is assumed to take place in autumn. The track is separated into 10 different sections starting at the stage grounds and ending at the finish line (Figure 2). At the staging grounds (a local football field), the helicopter must be able to fit in between the 40 yard lines when stationed at the 50 yard marker. There must be a minimum or 1 rotor radius clearance or 15 ft radius from all rotating components for ground crew safety. The 225lbs pilot has 10 minutes to warm up and 5 minutes to takeoff. The pilot is required to

Figure 2. Illustration of the course to scale on the Hudson River

start the course at no more than 100 kts. Then, the helicopter is required to perform 6 different maneuvers throughout the track. The full list of the racetrack course is displayed below.

Table 1: Complete list of mission segments.

Segment	0	1	2	3	4	5	6	7	8	9
Maneuver	Staging	Start	Slalom	Short Stop	Straight Away	Quad Pylon	Slalom	Hover, Pirouette Pickup	Side Flight	Finish
Altitude	<200 ft AGL	<200 ft AGL	<200 ft AGL	<500 ft AGL	<200 ft AGL	<200 ft AGL	<200 ft AGL	Sea Level	<200 ft AGL	<200 ft AGL
Temp	80°	80°	80°	80°	80°	80°	80°	80°	80°	80°

Each maneuver requires a certain amount of maneuverability and agility from the helicopter. For example, the slalom sections represent a series of sustained turns that require the helicopter to have a high maximum sustained load factor and a high roll quickness and control power characteristics at high airspeeds. The Hudson River course was broken down into 9 maneuvers and analyzed to determine the critical helicopter design parameters which would contribute the most toward reducing the overall course completion time. These maneuvers are illustrated in Figure 3. Speed, turning radius, load factor, control power, and acceleration/deceleration clearly became the most important characteristics for this racing rotorcraft.

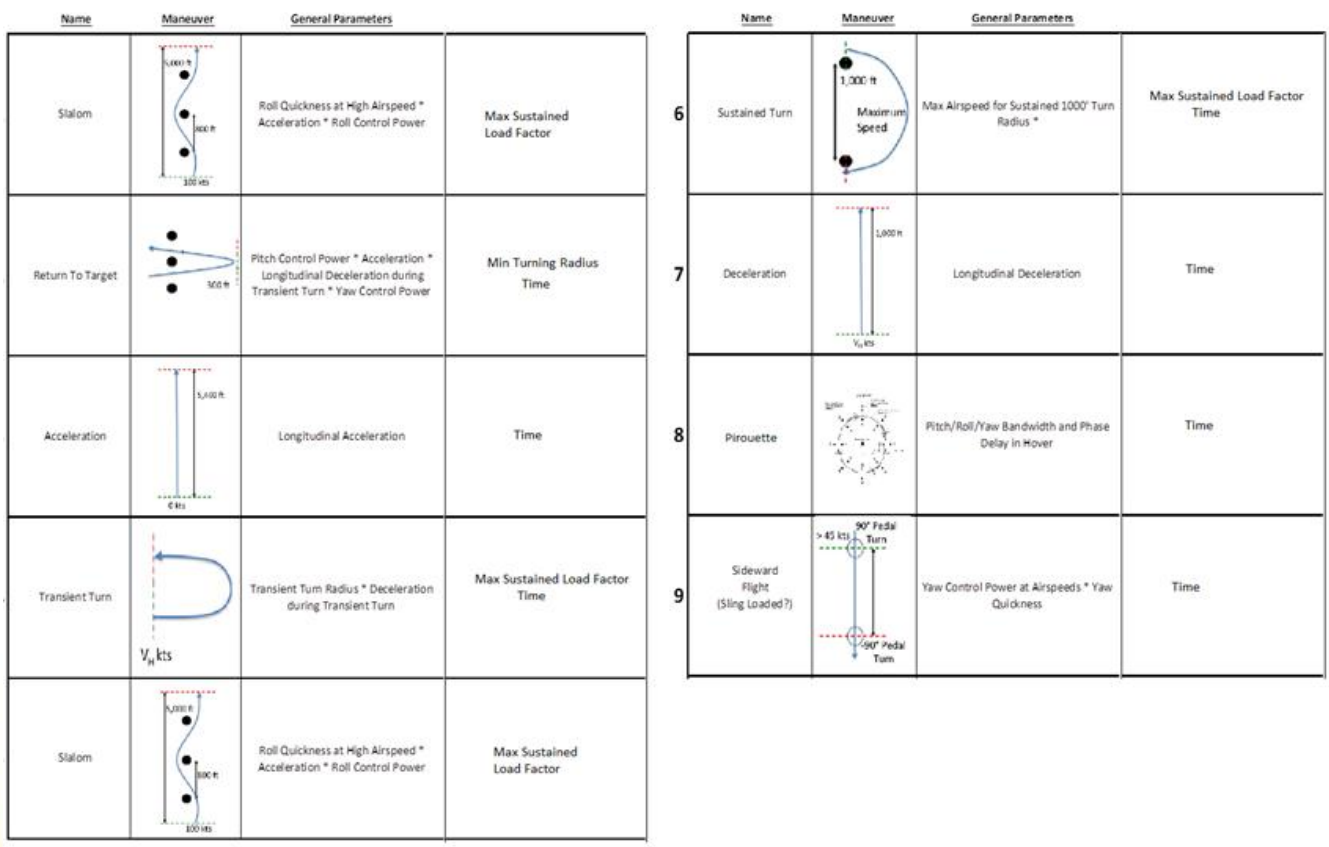

Figure 3. General Parameters associated with each maneuver.

GEORGIA TECH ROTORCRAFT CENTER OF EXCELENCE

2.2 Examination of Different Configurations

As with the design of any aircraft, it is important to determine what vehicle configurations provide the capability to perform the desired mission profiles. The team, therefore, decided to examine and compare the capabilities of the conventional helicopter, compound helicopters, tandem rotor helicopters, coaxial and intermeshing helicopters. In order to generate the advanced rotorcraft concept, a morphological matrix was generated. Table 2 shows that a total of 77,760 configurations options are available. From there, the list was narrowed down to 4 different configurations and a baseline model was chosen (Table 3). The Red Bull Messerschmitt-Bölkow-Blohm BO-105 was chosen as the baseline helicopter model since a model already exists for extreme maneuvering.

Table 2: Morphological Matrix

Category	Options						configurations
Rotor	Rotor Configuration	Single Main / Tail Rotor	Coaxial	Intermeshing	Tandem	Tilt	5
	Number of Blades	2	3	4	5	---	4
	Hub type	Articulated	Bearingless	Hingeless	Teetering	---	4
Configuration	Compound	Wing	No wing	---	---	---	2
	Vertical Stabilizer	Single	Dual	None	---	---	3
	Horizontal Stabilizer	Tail	Canard	None	---	---	3
Propulsion	Type	Rotor Only	Pusher Prop	NOTAR	---	---	3
	Number of engines	1	2	---	---	---	2
Landing gear	Type	Skid	Retractable	Water landing	---	---	3
Control	Type	Hydromechanical	Fly by wire	Fly by light	---	---	3

Total # of Configurations	77,760

Table 3: List of Chosen Configurations

Category		Baseline	1st Configuration	2nd Configuration	3rd Configuration	4th Configuration
Rotor	Rotor Configuration	Single Main	Coaxial	Intermeshing	Single Main	Intermeshing
	Number of Blades	4	4	3	3	2
	Hub type	Teeter		Teeter	Articulated	Teeter
Configuration	Type	No wing	No wing	No wing	No wing	No wing
	Vertical Stabilizer	Dual	Single	Single	Single	Single
	Horizontal Stabilizer	Tail	Tail	None	Tail	Tail
Propulsion	Type	Rotor Only	Pusher Prop	NOTAR	Rotor Only	Pusher Prop
	Number of engines	2	2	1	1	2
Landing gear	Type	Skid	Retractable	Retractable	Retractable	Skid
Control	Type	Hydromechanical	Fly by wire	Fly by wire	Fly by wire	Fly by wire

2.3 Analytical Hierarchy Process and Quality Function Deployment

"The secret to producing a successful helicopter is to let the requirements drive the design. When one comes in with an idea of a pre-design and attempts to tweak it for a successful requirement completion, one simply ends up with the wrong answer." – Steve Weiner (Sikorsky).

The previous words from the Chief Engineer for the Sikorsky X-2 and one of the 10 most brilliant innovators of 2009, according to *Popular Mechanics*, were kept in mind during the development for the design of what is now Georgia Tech's first intermeshing rotary wing racer. Establishing the evaluation criteria is therefore the first step in the analysis of the RFP requirements. Each requirement must be evaluated on their relative importance against the others. In order to determine what concept meets the objectives of the top level requirements, an analysis of different vehicle configurations is required.

To evaluate the different concepts and determine how each one of them meets the requirements, the Analytical Hierarchy Process (AHP) was used. This allows for the consideration of both objective and subjective opinions about various designs and the results provide relative weights that can be used in a Quality Function Deployment (QFD). The QFD is a populated matrix that compares relationship between design parameters on a nonlinear scale where a strong relationship (positive or negative) between the requirements is given a score of 9, a medium relationship has a score of 3, and a weak relationship has a score of 1. Thus, six different design criteria were chosen to represent the objectives of the RFP. These were then ranked based on the voice of the customer through a prioritization matrix as shown in Table 4.

Table 4: Prioritization Matrix

	Time	Fuel Burned	MRP	Safety Index	Acquisition Cost	Operational Cost	Ranking	RMS Fraction	Normalized %
Time	--	0.4	2	2.5	3	3	10.9	49.28%	24.0%
Fuel Burned	2.5	--	5	2.5	3	3	16	72.34%	35.2%
MRP	0.5	0.2	--	2.5	3	3	9.2	41.59%	20.2%
Safety Index	0.4	0.4	0.4	--	1.2	1.2	3.6	16.28%	7.9%
Acquisition Cost	0.33	0.33	0.33	0.9	--	1	2.9	13.11%	6.4%
Operational Cost	0.33	0.33	0.33	0.9	1	--	2.9	13.11%	6.4%

These four possible configurations were then subjectively evaluated with respect to these normalized weighted values based on engineering estimates and historical data. To help with this rating process, the single rotor configuration was used as the baseline, and the other configurations were evaluated based on whether they perform better or worse in each area. The results of this analysis can be seen below.

Table 5: Configuration Comparison

	Time	Fuel Burned	MRP	Safety Index	Acquisition Cost	Operational Cost
Single	1	1	1	1	1	1
Coaxial	1.3	0.8	1.3	1	1.5	1.5
Intermesh	1.1	0.9	1.3	0.9	1.6	1.5
Tilt Rotor	0.8	0.8	0.9	0.9	1	1

Combining the configuration comparison and the relative importance of each quality, TOPSIS, Technique for Order Preference by Similarity to Ideal Solution, was used to select an optimal configuration for the mission requirements based on an indisputable ranking method. TOPSIS involves defining "ideal" and "least ideal" configurations as the best/worst cross-configuration values for each characteristic. The ideal configuration values are normalized for each characteristic by the RMS for that characteristic.

Table 6: Normalized Configuration Comparison

	Time	Fuel Burned	MRP	Safety Index	Acquisition Cost	Operational Cost
Single	0.23	0.41	0.18	0.08	0.05	0.05
Coaxial	0.30	0.33	0.24	0.08	0.07	0.08
Intermeshing	0.25	0.37	0.23	0.08	0.08	0.08
Tilt Rotor	0.19	0.33	0.16	0.08	0.05	0.06
OPTIMAL	0.30	0.41	0.24	0.08	0.08	0.08
WORST	0.19	0.33	0.16	0.08	0.05	0.05

The radar plot shown in Figure 4 shows the worst configuration in red and the ideal in blue to show graphically in what range the configurations can fall. It is clearly shown that there is little to be gained or lost for the mission with respect to safety concerns, but a lot can be gained where time, MRP, and fuel burned are concerned.

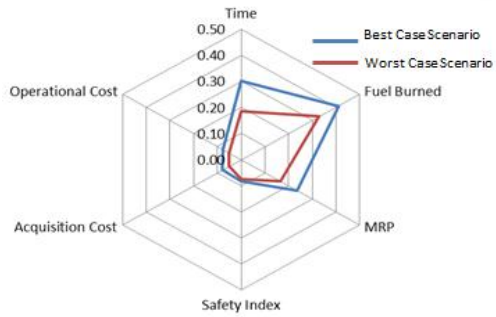

Figure 4. Ideal Configuration

The next step in TOPSIS selection is to determine how close each configuration is to the ideal and how far each configuration is from the worst. This "separation factor" is taken to be the RMS of the differences between real and ideal/worst, and these values are used to calculate a "closeness factor" by dividing worst separation by ideal plus worst separation (the maximum value being 1). A radar plot showing how each configuration fared with respect to the ideal case can be seen in Figure 5.Finally, their normalized relative separation and closeness factors can be seen in Table 7 below.

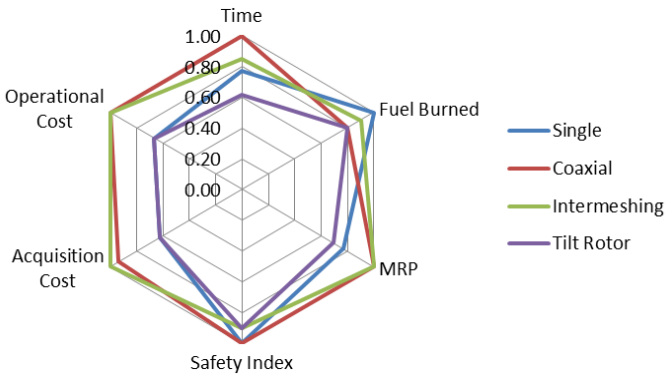

Figure 5. Configuration Comparison Radar Plot

Table 7: Closeness Factors

	Separation+	Separation-	Closeness
Single	0.10	0.10	0.50
Coaxial	0.08	0.14	0.63
Intermeshing	0.06	0.12	0.65
Tilt Rotor	0.16	0.01	0.06

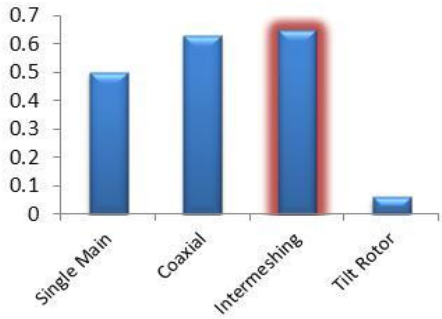

Figure 6. TOPSIS Results

Based on the TOPSIS methodology and engineering estimates, the intermeshing rotor configuration was chosen as the best fit for this particular mission. Figure 6 shows that the coaxial rotor was a very close second. That being said, the preliminary design conducted led to the intermeshing design concept, taking into consideration that the RFP grading included a section for originality. This design is the first synchropter design to come from Georgia Tech and is commonly known as unconventional for highly maneuverable aircraft. All things considered, it was concluded that the intermeshing design was the most original and optimal configuration for this mission and competition.

Table 8: Quality Function Deployment

				Engineering solutions															
				Maneuverability and Agility Design Parameters						Mechanical Design				Performance Parameters					
		Non Linear Scale 1 - Weak Relation 3-Medium Relation 9 - Strong Relation	Weight of Parameter (1 - 5)	Installed HP	Lock Number	Disk Loading	Blade Loading	Solidity	Tip Speed	Transmission	Power Loading	Material Selection	Avionics	Gross Weight	Flat Plate Drag	Rotor Radius	Load Factor (G)	Acceleration	Autorotrative Index
		--	--	▼	▼	▲	▲	▼	▼	▼	▼	▲	▲	▲	▼	▼	▼	▼	▼
Engineering Requirements	Operational Requirements	HOGE 103F	5	9	3	9	9	9	3	1	9	0	0	9	0	3	0	0	0
		125knot @ 90% MCP	5	9	3	3	3	3	3	1	9	0	9	3	9	3	1	1	0
		225 lb Pilot	3	3	0	3	3	3	0	1	3	0	0	1	1	1	0	0	0
		Slung Load Capable	5	9	3	9	9	1	1	1	9	3	3	3	0	1	1	0	0
		60knot Sideward Flight	5	9	3	3	1	3	0	0	9	0	1	3	9	1	3	0	0
		Foot Print	3	3	0	1	1	3	3	1	1	0	0	1	9	9	0	9	0
		Course Time	5	9	1	3	3	3	3	\1	9	0	1	9	9	3	9	9	0
	Performance	Maneuverability	5	9	9	9	9	9	9	1	9	0	3	9	3	9	9	9	0
		Agility	5	9	9	9	9	9	9	1	9	0	3	9	3	9	9	9	0
		Acceleration	4	3	3	9	3	3	1	1	9	0	9	9	3	1	9	9	0
		Forward Flight Speed	4	9	3	3	3	9	9	0	9	0	3	3	9	9	3	1	0
		Engine SFC	5	3	0	1	3	3	1	3	3	0	9	9	3	1	0	9	0
		MRP Required	4	0	0	3	3	9	3	1	9	0	1	9	9	3	9	9	0
	Safety	Autorotation	3	0	9	9	9	9	9	9	0	3	1	3	1	9	0	0	9
		Crashworthiness	2	0	0	0	0	0	0	9	0	9	0	3	0	3	1	0	9
		Survivability	2	0	0	0	0	0	0	9	0	9	0	3	0	1	1	0	9
	Cost	Acquisition Cost	1	3	0	1	1	1	0	3	1	3	3	3	1	1	1	3	0
		Operational Cost	3	9	0	0	0	0	0	3	3	1	1	1	0	0	0	3	0
		Maintenance	1	3	0	0	3	0	0	9	3	3	1	1	0	0	0	3	0
		Overall Efficiency	4	9	1	3	3	3	3	3	3	1	1	9	0	3	1	3	0
			Raw Score	465	117	342	321	342	245	155	475	73	211	424	298	280	253	315	63
			Scaled	1062%	267%	781%	733%	781%	559%	354%	1085%	167%	482%	968%	681%	639%	578%	719%	144%

2.4 Configuration Trade-off

This section assesses the relative merits of the Single Main Rotor, Coaxial Rotor, and Intermeshing Rotor Configurations.

General Comparison

Table 9 shows a configuration comparison centered on the intermeshing configuration.

Table 9: Advantages and Disadvantages of Intermeshing Configuration

Comparing Intermeshing to:	Advantages of Intermeshing	Disadvantages of Intermeshing
Single main	• No tail, more power for main rotors. • True lift symmetry. No asymmetry in forward flight. • No tail, smaller fuselage length. • Very easy on the pilot.	• Higher drag. • Deficiencies with respect to yaw control
Coaxial	• No limitations due to risk of blade tips striking each other. • Significantly simpler transmission. • True lift symmetry in forward flight. • Better sideward flight due to canted rotors. • Very easy on the pilot in terms of controls.	• Slightly larger footprint and width. • Lost lift due to canted rotors (~2%).

Power Efficiency

Table 10 supplements the discussion in this section. The following correction relations from Leishman's *Principles of Helicopter Aerodynamics* were used for the intermeshing and coaxial configurations to produce the following equations.

$$\frac{P_{i_{tot}}}{P_i} = K_{ov} = 1 + \left(\sqrt{2} - 1\right)m = 1 + .4142m$$

$$where: \quad m = \frac{2}{\pi}\left[\theta - \frac{d}{D}\sin\theta\right] \quad and \quad \theta = \cos^{-1}\left(\frac{d}{D}\right)$$

Table 10: Configuration Characteristics Based on Momentum Theory.

Rotor Configuration	Single	Coaxial	Intermeshing
Relative Ideal Power Required, Constant Thrust (efficiency measure)	1	1.414	Between 1 and 1.414
Relative Maximum Thrust, Constant Power (efficiency measure)	1	1.414	Between 1.414 and 2
Relative Geometric Solidity (efficiency measure)	1	2	Between 1 and 2
Relative Thrust-Weighted Solidity (blade loading measure)	1	2	2
Relative Maximum Blade Loading, Stall-Limited (blade loading measure)	1	2	2

Lift efficiency is better for the intermeshing rotors than the coaxial rotors on the basis of induced velocity and solidity trends, while blade loading is not penalized.

A coaxial rotor configuration's bottom rotor operates in a developed (and thus high-velocity) slipstream wake, because the coaxial rotors are right on top of each other and must have considerable vertical distance between them due to tip collision concerns. Therefore the overall induced velocity from the coaxial helicopter has to be greater than that of an intermeshing configuration to achieve similar thrusts and therefore the efficiency is lower. Figure 7 depicts how the Figure of Merit (FM) of the bottom rotor of a coaxial prop-rotor is hurt by the additional induced velocity.

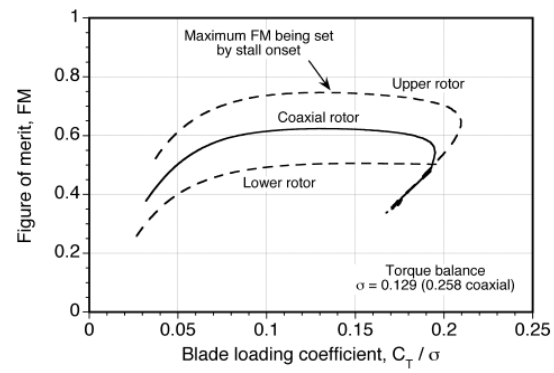

Figure 7. Discrepancy in performance of the two rotors in a coaxial prop rotor.

The bottom rotor of a coaxial operates at a much lower FM due to being in a very developed slipstream. The intermeshing rotors do not operate in a developed slipstream, and thus each would operate closer to a single rotor FM.

In the intermeshing configuration geometric solidity cannot equal thrust-weighted solidity as it does for non-tapered single main rotors. Helicopter rotors become more efficient the larger they get, due to intake of a larger volume of air leading to lower induced velocity and lower blade interactions. For these reasons it is observed that higher geometric solidity tends to decrease efficiency, and here the effective solidity is higher in the coaxial than in the intermeshing (the coaxial has full overlap whereas the intermeshing has partial overlap). An important parameter in maneuverability and agility is the blade loading coefficient (thrust coefficient normalized by thrust-weighted solidity). The primary objective of this parameter is to discern the maximum excess thrust a helicopter can use for maneuvers, limited by stall rather than power. A higher thrust-weighted solidity increases the value of this parameter due to blades having to operate at lower angles of attack for larger lifting surfaces and thus delaying stall with respect to collective pitch increase. This must be for thrust-weighted solidity, rather than geometric solidity, because the thrust generated is limited by the stall point. For non-tapered blades the geometric and thrust-weighted solidity are the same for the coaxial and single main rotor configurations, but for the coaxial configuration the geometric and thrust-weighted solidity are different. The thrust-weighted solidity in intermeshing rotors is simply double that of a single rotor, because the thrust is equal on both rotors. Therefore the relative maximum blade loading are roughly equivalent for the coaxial and intermeshing configurations.

Synchropter's Maneuverability and Agility Capabilities

This analysis aims to isolate the effect of the intermeshing configuration. Suppose blade geometries are the same in all configurations. The single main rotor configuration (SMR) has four blades, while the coaxial rotors configuration (CR) and intermeshing rotors configurations (IR) each have two rotors of two blades each. This way the total solidity if the rotors were 'stacked up' would all be equal to each other.

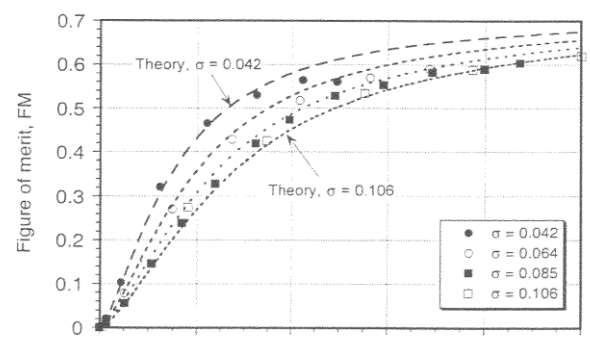

Figure 8. FOM vs. Thrust Coefficient for Different Solidities from Experiment and Theory.

Viewed from above the helicopters, the solidity of the CR and SMR are the same. An adjusted solidity for the IR can be calculated to be the intermeshing fraction-weighted solidity, where the intermeshing areas have the same solidity relative to the SMR and CR, and the regions outside the SMR have half of this relative solidity. For the K-MAX this solidity turns out to be about 10% lower. The total projected disk area increases (where the SMR and coaxial have the same), and for the K-MAX this turns out to be about 10% higher. These changes can be tweaked to be much larger by varying rotor disk size and orientation and height of the rotor hubs. For reasonable mast heights and orientations and rotor sizes, disk area increases of 20% and solidity decreases of 20% were easily obtained.

For both reasons of solidity and disk area, the IR benefits in terms of maneuverability and agility. These performance characteristics rely on blade loading margin. The blade loading structural limit stays the same among the different configurations, since the blade geometry and structure are the same. The increased disk area in IR allows for a lower operating blade loading, and thus an increased blade loading margin. The lower solidity leads to a higher figure of merit at a given thrust coefficient, meaning a higher efficiency. This allows for a lighter and smaller, and thus more agile, aircraft.

It is common to associate a higher solidity with better maneuverability and agility. However, this arises from blade stall considerations and assumes an increase in solidity by an increase in blade chord. An increase in blade chord means the angle of attack can be lower for a given operating condition and thus the margin for increase of angle of attack before stall is increased. The intermeshing achieves a lower effective solidity by virtue of rotor configuration, for the same blade geometry. Therefore, the maneuverability and agility in the IR is not penalized for stall constraints, even though the solidity is lowered and FOM is increased. Figure 8 shown above illustrates this relationship (Leishman).

Forward Flight

The coaxial and intermeshing rotors have a huge advantage over the single main in thrust margin at high speeds, because the lift distribution on the single main rotor becomes heavily asymmetric and the helicopter will tend to roll over, adding to stall and power limitations on the thrust produced at forward speeds. This is very important for the current mission and perhaps important enough to be enough reason alone to choose one configuration over the other. The coaxial lift distribution is still not symmetric, as the two rotors operate under different aerodynamic conditions resulting in significantly different figures of merit, as has been discussed. The synchropter, however, has a perfectly symmetric lift distribution in forward flight. Thus it can be expected that in forward flight the synchropter is superior to the coaxial on the basis of available thrust margin and lower controls requirements. This translates to higher thrust margin in forward flight, lower pilot load, lower controls load, and better maneuverability for the synchropter over the coaxial helicopter.

3 PRELIMINARY SYNCHROPTER SIZING

3.1 Weight Sizing

Vehicle weight is a critical component in rotorcraft design, affecting every aspect of its performance. It was therefore necessary to estimate the total component weights of the synchropter at each stage of design in an iterative process form, ultimately converging upon an accurate measurement of vehicle weight that could be used in driving other design processes.

3.2 Method

The RF method (or fuel required method) was the primary tool used to approximate the Badger's weight. A Python code was used to implement the RF method algorithm due to its speed, simplicity, and wide usage.

The method as an iterative process considers the mission requirements, vehicle characteristics, and empty-to-gross weight ratio, combined with historical trends, and outputs fuel weight, vehicle weight, and engine power required. Thus, it is easily seen how individual vehicle characteristics affect the overall requirements of the aircraft in terms of weight and power. The mission requirements were taken from the RFP competition course, and specific performance specifications were prescribed as goals, including dashing at 160knots, 3 g's of acceleration, and sling load dashing. The program calculates the maximum required power and the power required for each mission segment. This in turn is used to calculate the fuel required for each segment, which must add up to (at most) the fuel available. If the fuel available is insufficient, the process is repeated with more until a solution converged, keeping in mind fuel reserves.

This process was repeated and modified at every step of design to account for the additions and changes made. The weight outputs at each stage were then used as bases for further change and additions. This

process continued until our final design, where we kept our final weights and performance metrics. A weight breakdown was created by combining the Rf method's gross and empty weight approximations with empirical formulas for component weights as well as more exact weights when possible (e.g. the known weight of our hook, cockpit equipment, etc.)

3.3 Results

From these results we were able to approximate the performance of our helicopter through the competition course as well as perform structural analyses to check the safety of our design. By several iterations of the R_f method and historical data, we were able to size our helicopter at 2500lbs with 127lbs fuel (Jet-A) for this course. The fuel weight includes the required 15 minutes of fuel reserve. The weight breakdown can be seen in Figure 9 & Table 11.

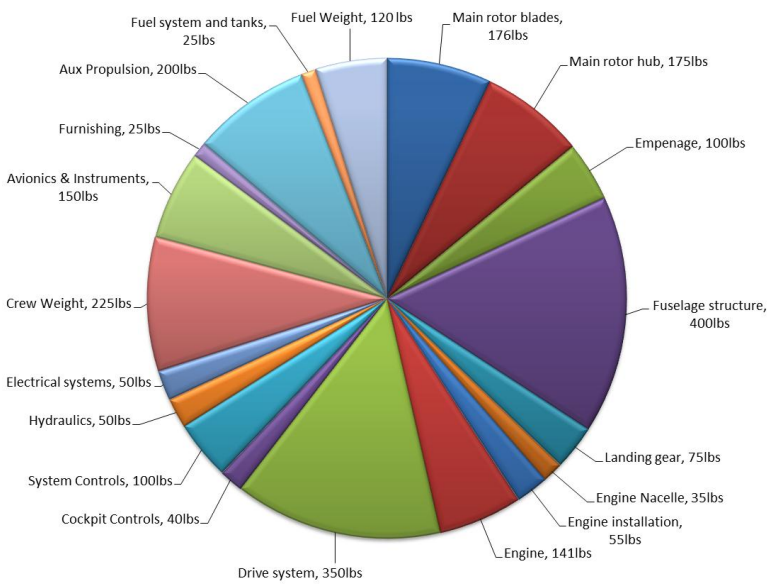

Figure 9. Component Weight Breakdown Pie Chart

Table 11: Component weight breakdown

Component	Weight (lbs)
Main rotor blades	176
Main rotor hub	175
Empennage	100
Fuselage structure	400
Landing gear	75
Engine Nacelle	35
Engine installation	55
Engine	141
Drive system	350
Cockpit Controls	40
System Controls	100
Hydraulics	50
Electrical systems	50
Crew Weight	225
Avionics & Instruments	150
Furnishing	25
Aux Propulsion	200
Fuel system and tanks	25
Fuel Weight	127
Gross Weight	**2499**
+300lb Slung Load	**2799**

4 MAIN ROTOR DESIGN

4.1 Blade Radius

The first step in defining the main rotor is to find an acceptable disk loading value. From a qualitative standpoint, a high value in disk loading (DL) is unwanted since it causes severe consequences in hover conditions. As the DL increases, higher downwash velocities are produced. This will then create a safety hazard to ground crews in area. Since the Badger is required to lift off from a very busy football field, there is a limited amount of space in the safe ground operations (15 feet from all moving components). Also, a high disk loading value will increase the power required by the main rotor.. On the other side of the spectrum, the lower the disk value is, the better the maneuverability will be. A low DL produces better acceleration characteristics, a reduced tip speed for a constant blade loading, and better autorotational characteristics. Therefore, when designing a main rotor for maximum maneuverability, the disk loading needs to be as low as possible.

The lowest value of disk loading is bounded by the maximum size of the rotor's radius. The most constricting requirement on the maximum radius is the ability to safely enter the pylon gates. Figure 10 and Figure 11 illustrate geometric constraints set by the pylon gates. In Figure 10, a set of dashed gray lines represents soft safety margins that will provide the pilot with an acceptable amount of

maneuverability. When the helicopter flies at the suggested location (10.5ft from the pylon at an altitude of 45ft from the helicopter's blade tip) the maximum rotor radius becomes 12.4ft creating a disk loading of 2.58lbs/ft^2. This optimum window allows the pilot to have a rotor clearance of 6.5 ft from both sides and 10 ft above and below penalty and caution zones.

The RFP states that the staging for the event will take place at a local football field. The helicopter must have a 15ft safety zone around all rotating components for safe ground operations. It must also fit in between the forty yard lines at the center field. With a 12.4ft radius, the synchropter meets this criterion. Figure 12 illustrates the safety zone radius around all moving parts, including the aux propulsion system.

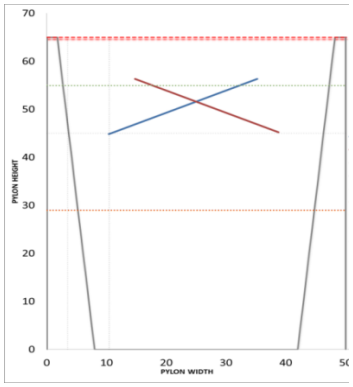

Figure 10. Maximum Radius to obtain 7ft of clearance from either pylon

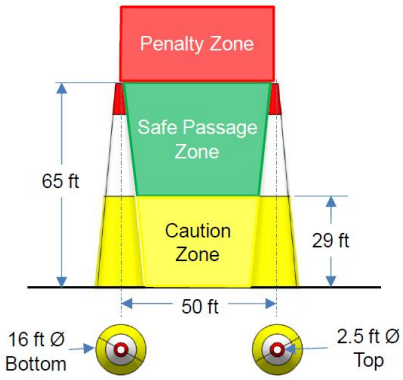

Figure 11. Illustration of pylon dimensions given from the RFP

Figure 12. 15ft safety clearance around all moving parts, drawn to scale

4.2 Aspect Ratio

From historical data, typical aspect ratios of helicopter blades will range from around 15 to 20. The majority of light weight configurations will have higher aspect ratios to reduce blade weight and drag. The smaller chord length also has a positive effect on reducing the power required curve. However, if the chord is too short, it can jeopardize the stall margin and structural strength of the beam. Generally, blade chords are designed to be no less than 6 inches. Figure 13 illustrates a handful of chord lengths from current helicopters. The historical data proves that as helicopters decrease with weight, the chord becomes smaller boarding the 6 inch limit. Thus, light weight helicopters have higher aspect ratios blades. Therefore when designing the Badger's main rotor blade, the blade aspect ratio should be designed to reach 18-20. The final aspect ratio was defined to be AR=19. The red dot in Figure 13 is the Badger's aspect ratio in comparison to the historical data.

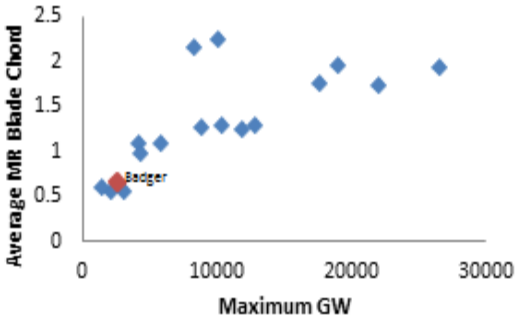

Figure 13. Historical trends of the blade chord lengths as a function of gross weight

4.3 Tip speed

In order to maximize the maneuverability of a helicopter, the rotor should be designed to have a very high tip speed. This is because high tip speeds reduce the angle of attack on the retreating side of the rotor disk and remove the problem of the blades stalling out. It also produces better autorotational characteristics which is a safety requirement in the RFP. The main limit for high tip speeds is the drag divergence that occurs as the blade tips reach the transonic Mach regime. Figure 14 illustrates how tip speeds can only range from 400-750 due to several boundaries such as the compressibility limit as previously mentioned, noise limit, and stall limit (Leishman). This graph assumes that the drag divergence Mach speed is 0.92. This limit is only possible with the use of advanced chord concepts such as the ones used in the British Experimental Rotor Program (BERP). For simplicity and cost, the Badger does not incorporate any experimental tip shapes. Therefore, the Mach divergence limit will be a lower number. Based off the VR7B airfoil performance (Figure 15) and assuming that the blades would have zero to three degrees pitch at the tip, will set the airfoil divergence number at 0.85. With the Badger's maximum speed at 170 kts, the highest tip speed possible is 670 ft/s.

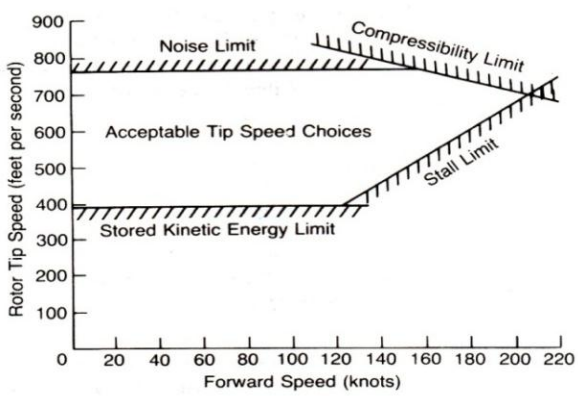

Figure 14. Range of acceptable tip speeds

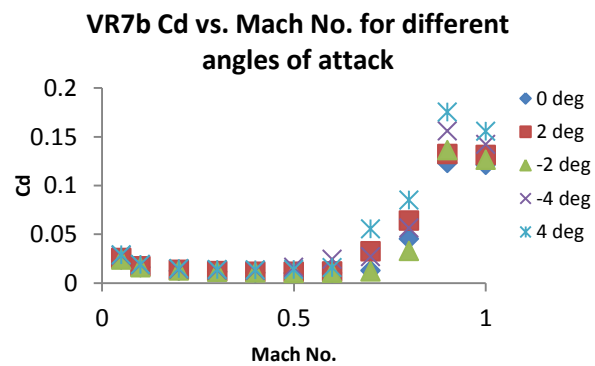

Figure 15. Drag characteristics of the VR7B airfoil

4.4 Number of Blades and Chord length

For a helicopter of the Badger's size and mission requirements, a blade designed with taper and nonlinear twist would not benefit enough to offset the high cost of production of such a complex blade (Johnson). Furthermore, this simplification allows for an optimization procedure using blade element momentum theory (BEMT), which is discussed in the next section on twist optimization.

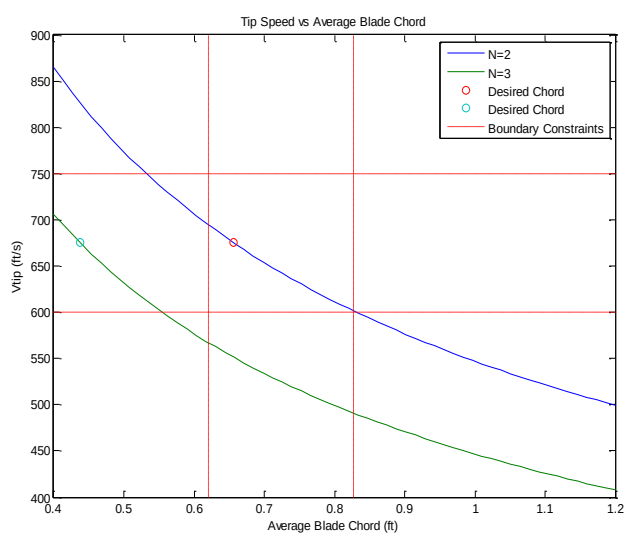

Figure 16. Acceptable chord lengths for tip speeds ranging from 600 to 750 ft/s and aspect ratios from 15 to 20

Since the chord length remains constant throughout the span, finding an acceptable chord became relatively simple. In the above sections, some of the variables necessary for designing a rotor disk were assigned. These parameters being a high aspect ratio blade, blade radius of 12.4 ft, and tip speed of 670 ft /s. The next step was to set a designed thrust to be produced at hover. Each rotor was set to achieve 1.15*(GW/2) pounds of thrust at a $C_t/\sigma<0.2$. Figure 16 represents the possible chord lengths that can satisfy the boundary conditions previously described (AR_{min}=15 AR_{max}= 20 $Vtip_{min}$=600 fps $Vtip_{max}$=750 fps). The C_t/σ was varied to give the configuration with

the highest aspect ratio. The final chord dimension produced a aspect ratio of 19, thus satisfying the maneuverability condition. Therefore, C_t/σ of 0.085 produced the only acceptable chord length at 0.66 ft.

In Figure 16, it is also very easy to see how a 2 bladed system is the only acceptable configuration. Three blades cannot satisfy any of the conditions needs. With the knowledge available, the team concluded that three blades would increase the main rotor weight power required and fuel weight for the same aspect ratio blade. In conclusion, the dimensions of the main rotor disk are listed in Table 12.

Table 12: Dimensions of main rotor disk

Blades per rotor	2
Disk Loading (lbs/ft²)	2.58
Radius (ft)	12.4
Chord (ft)	0.66
Tip speed (ft/s)	670
Aspect Ratio	18.6

4.5 Twist Optimization Procedure

A blade element momentum theory (BEMT) code written by Robert Scott, a graduate student at Georgia Tech, was heavily modified to provide a basis for determining the rotor blade geometry of the GT-Badger. The goal was to use BEMT to determine the rotor configuration with maximum thrust margin in hover given maximum engine power (determined by sizing methods) and stall limits (determined by the C81 tables). The thrust margin was optimized for twist, given a power limit. This was a combined measure of resistance to stall with higher thrusts and efficiency.

Approach

The goal of this BEMT analysis was to find the twist and airfoil section that optimized thrust margin given a set of other parameters initialized by other factors. Some of these factors included tip speed, which was kept within a window of practical values, rotor radius, which was constrained by pylon clearance, and engine power, which was dependent on other sizing factors. These parameters however can be changed iteratively for the purpose of increasing thrust margin, since thrust margin is a very important consideration for the current mission.

The blade geometry was simplified to have constant chord and linear twist, because nonlinear twist and taper are cost-justifiable only for large helicopters and for a helicopter of this size does not impart significant improvement. Also, each rotor configuration utilized a single airfoil section. Although the airfoil and chord distributions were simplified, the code was written so that more complex distributions can be easily defined, if need be. All of the initialized parameters are detailed and summarized in Table 13.

Table 13: Parameters Initialized by Other Considerations

Parameter	Value	Driving Factors (Effect on Value)
Number of blades per rotor	2	Power consumption (decrease), safety (decrease)
Rotor radius (ft.)	12.4	Pylon clearance (decrease), tip speed (increase), efficiency (increase)
Tip speed (ft/s)	685	Drag divergence (decrease), maneuverability (increase), lift (increase)
Aspect ratio	20	Economic reasons, simplicity, practical aspect ratio, solidity (increase)
Max power per rotor	200	Gross weight (decrease), lift (increase)

On the order of thousands of BEMT runs were completed for each optimization trial, which found the root pitch and total linear twist of maximum thrust margin, given the other parameters. For each total linear twist, the highest thrust margin was found by varying root pitch. Then, the maximum thrust margin for a linear twist was taken to be the optimum configuration. Figure 17 and Figure 18 are representative of the thrust margin vs. twist and root pitch:

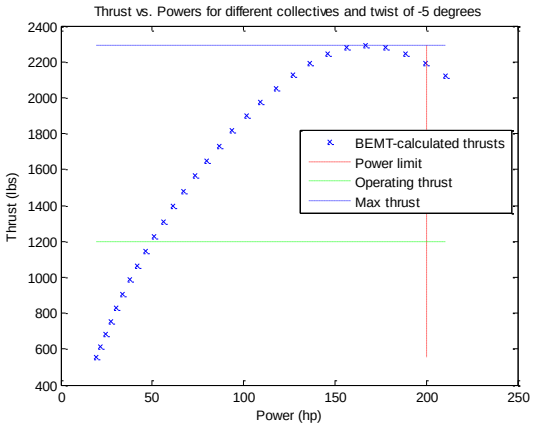

Figure 17. Representative Plot of Optimizing Thrust Margin for a Given Total Linear Twist

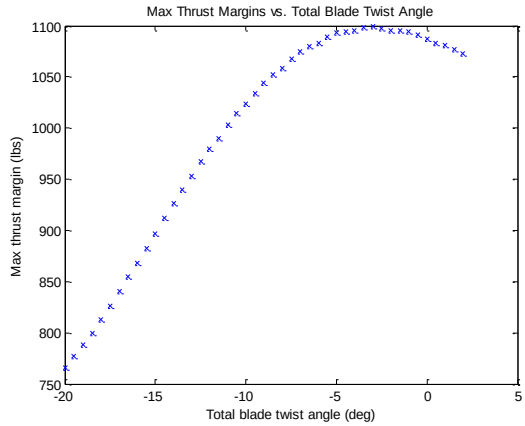

Figure 18. Optimization Plot Max Thrust Margin with Respect to Linear Twists, whose Maximum Thrust Margins were Found in a Manner as Shown in Figure 12

Results

The characteristics for the baseline rotor optimized for thrust margin are outlined in Table 14. Each configuration was tested using a single airfoil, and all of the available C81-tabularized airfoils were tested. The one with the resulting maximum thrust margin was chosen. Maximum thrust margin was a measure of stall resistance to increased thrust and efficiency. These hover power figures were calibrated with the power code to set the power required in hover.

Table 14: Baseline Rotor Optimized by Thrust Margin

Total blade twist (degrees)	-10.5
Root pitch at operating condition / zero collective (degrees)	10.6246
Tip pitch at operating condition / zero collective (degrees)	0.1246
Airfoil	VR7B (tabbed)
Operating thrust (lbs.)	1250 (x2 rotors = 2500 total)
Power required (hp)	89.5 per rotor, 179 hp total

4.6 Airfoil Sections

A main rotor airfoil was chosen through optimization of thrust margin for a given rotor design parameters (those discussed previously). For each airfoil available in the C81 tables, twist was optimized so that the maximum thrust margin was found, and this was associated with the airfoil. The airfoil allowing for the highest thrust margin was chosen. This turned out to be the VR7b tabbed airfoil. Using the twist optimization procedure to choose an airfoil proved very effective, as the thrust margins for different airfoils was observed to be up to a factor of 2 apart. The other airfoils tested were: FX69H083, FX69H098, OA206, OA209, OA213, SC1094R8, SC1095, SC2110, VR5, VR8, VR9, VR13, VR14, and the VR15. All airfoils with C81 tables available were tested.

5 HUB DESIGN

The first step in designing the Badger's hub was choosing a specific type. Three different hubs were qualitatively investigated: teetering, articulated, and rigid. Each hub was given a rating of 1 (the worst score) to 5 (the best score) for several characteristics deemed important qualities for this mission. As concluded by the team, the best hub system would be simplistic, low weight, most applicable for a two

GEORGIA TECH ROTORCRAFT CENTER OF EXCELENCE

bladed rotor, and have a low hub stress. Figure 19 compares the results of the three different systems. An under-slung teetering rotor was deemed the best hub choice.

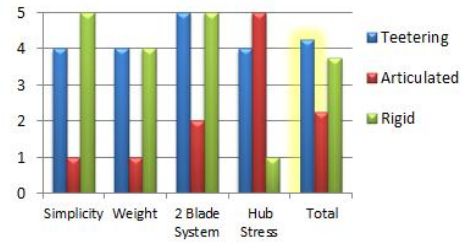

Figure 19. Qualitative hub system assessment

It is extremely important to note that the teetering system without any modifications would not provide adequate control power and maneuverability characteristics. Without the inclusion of a hinge offset, the teetering rotor does not produce any hub moment in low and zero-g flight. To provide an equivalent hinge offset, a hub spring must be included. A hub spring is a system which isolates the two-per-rev hub spring moment vibrations while providing control power during zero-g flight. The hub spring structure is connected between the rotor and the mast to resist rotor flapping about the teeter axis. Increasing the hub spring moment coupling between the main rotor and mast will increase control power about the pitch and roll axes. This will thereby provide the necessary increase in maneuverability and c.g. range. For the Badger, the spring is 6 % of the hinge offset Equivalence. The hub spring for the Badger was modeled directly off of the third modification of Patent #4333728 "Compound hub spring system for helicopters" by Jan M. Drees et al. The spring provides a linear resistance at low flap angles and higher nonlinear spring rate for the removal of mast bumping characteristics between the rotor and mast. The hub spring system utilizes a tapered elastomeric snubber block and elastomeric shear pads to provide the resistive flapping force. The resilient snubber block provides the nonlinear restraining force from its tapered shape. If the flapping angles are low, the smaller tip of the block produces a minimal amount of resistive force. As the flap angle increases, the contact area's deformity increases between the coupled mast and rotor blade yoke creating a much larger force. The four elastomeric shear pads in the compound system create a flap-opposing shear bias that is linearly proportional with the flapping angle. An illustration of the hub spring design is shown in Figure 20. Views of the hub spring system from patent (first row) and hub spring on The Badger (bottom row). The teetering hub will still remain relatively simplistic since the hub spring removes the necessity of lead-lag dampers.

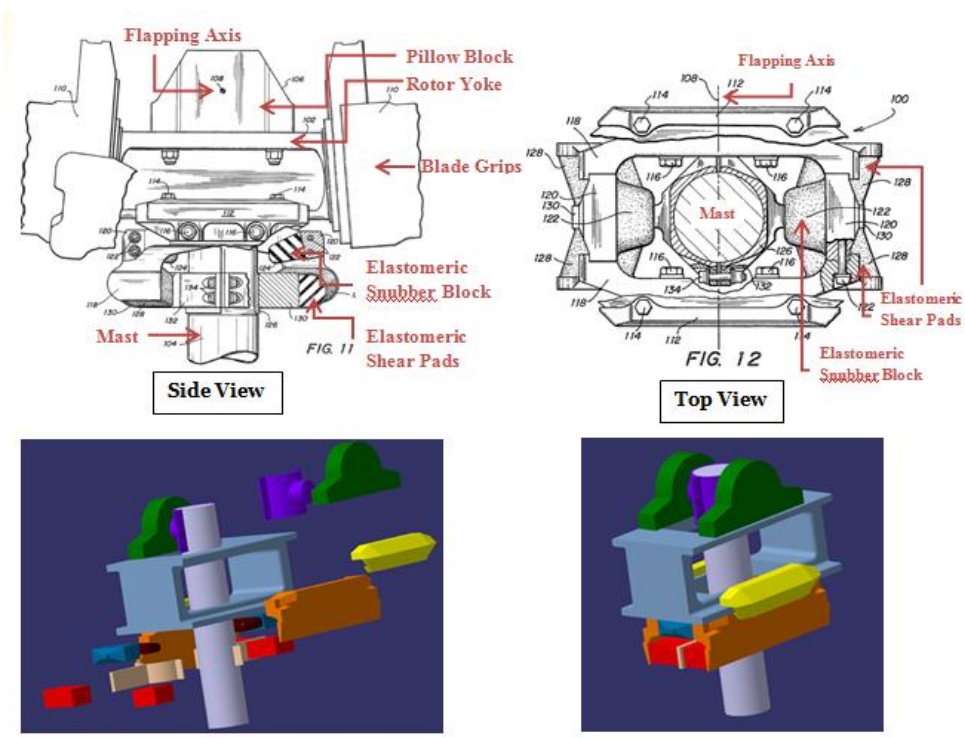

Figure 20. Views of the hub spring system from patent (first row) and hub spring on the Badger (bottom row)

Collective and cyclic control is produce by servo flaps (Figure 21). These flaps placed 75% down the blade span, act similarly as an airplane's elevator. When the servo flap is deflected, it uses energy drawn from the air-stream to pitch the blades up and down. The servo flap then twists the blade to the requested angle of attack. It drastically simplifies the teetering hub by replacing the need for pitch link arms and a swash plate. It uses a light control linkage instead of the typical heavy hydraulic system, since the control forces only need to be large enough to deflect the small flaps. Servo flaps also dampen out vibrations. In previous Kaman models, the blades were designed to have a soft torsional root to allow blade pitch (Singh). However, since the Badger will be performing an intense series of maneuvers the hub has a feathering bearing instead so the blade's material stiffness can be increased.

Figure 21. Servo flap on the Kaman K-Max

To remove the possibility of the blades striking each other and the neighboring mast and hub, the hubs must be laterally tilted 13° creating a total angle between the shafts of 26°. This deflection was chosen because the maximum amplitude of combat helicopters is of the order of 13° while civil commuting aircraft is 10° (Tischenko). Although the Badger is neither a combat nor a civil helicopter, it can be assumed that the maneuver through this race course can be the equivalent of a combat helicopter's nap of the earth flight. This design is just like the Kaman K-Max which has a total angle of 25° between the masts. The blades are also built with 1° of pre-cone, also following the trend of typical teetering rotors.

6 PROPULSION

6.1 Engine Sizing

Several different criteria were considered when sizing the engine:

- Must be able to fly at least 120 knots at 90% MCP.
- Must be able to pull a 3g turn (maneuvering consideration).
- Must be able to fly 60 knots sideways.
- Must minimize the Eta Function by finding the minimum MRP required and minimum fuel consumption.

To see if the aircraft could fly 120 knots at 90% MCP, equations were taken from the Engineering Handbook 706-201, in addition to the flat plate drag obtained from empirical and CFD results, to analyze the drag created in forward flight and the power required to counteract it. The next criterion analyzed was the 3g turn. An equation was found in the Handbook for a single rotor helicopter and modified for an intermeshing. The equation used is displayed below where K is the intermeshing correction factor.

$$n = \sqrt{1 + \frac{550hp_{extra}}{W_g v_{eq} \kappa}}$$

Using this equation, the MRP was varied until the load factor capability of the vehicle was approximately 3g's. This MRP level exceeds the first condition making this criterion the determining factor for engine sizing. When this equation is coupled with the forward flight calculations, the load factor capabilities of the aircraft can be found. Figure 22 shows the load factor capability of the rotorcraft in forward flight. The engine size was also checked against the sideward flight requirement and found to work. Figure 22 shows the final engine sizing.

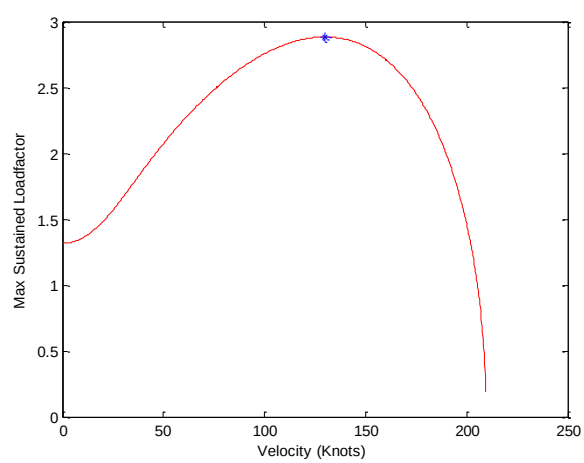

Figure 22. Load factor capability in forward flight

After determining the 550hp designed MRP, the equations given in the RFP were used to scale the engine's performance for off design atmospheric conditions and power ratings in order to meet engine performance and requirements.

Table 15: Engine Performance

	SL/ISA		SL/103F		6K/95F	
	HP	SFC (lb/hp*hr)	HP	SFC (lb/hp*hr)	HP	SFC (lb/hp*hr)
OEI	703.6	0.378	581.5	0.392	474.2	0.390
MRP	672.1	0.379	550.0	0.396	445.4	0.395
IRP	626.5	0.384	508.4	0.403	409.8	0.402
MCP	512.4	0.398	415.2	0.424	338.0	0.422
Part Power	336.0	0.448	275.0	0.490	222.7	0.486
Idle	134.1	0.706	110.0	0.824	89.2	0.816

Table 16: Fuel Distribution

Segment	Fuel (lbs)
Warm-up	5
Race	67
Auxiliary	55

Once the Engine Performance was established, the team was able to confirm the fuel required for each section. This is shown in by Table 16 shown to the right. These values are based on approximations by carefully evaluating each segment of the race and assuming a corresponding SFC.

One Engine vs Two Engines Trade Study

A simple study was conducted using the equations provided in the RFP. The results showed that one engine was found to be more fuel efficient and lighter than having two engines. Table 17 shows a synopsis of the comparison.

Table 17: One Engine vs. Two Engines

Number of Engines	1	2
Weight (lbs)	113.1	143.4
MRP SFC @SL/ISA	0.396	0.434

6.2 Auxiliary Propulsion Study

Auxiliary Yaw Control

An initial look at the rotorcraft's projected racetrack would suggest that the rotorcraft would need an exemplary yaw control ability to have maximum maneuverability and agility. The red portions of Figure 23 are the sections in which the maneuvers require a high lateral-directional control. The most stringent lateral-directional maneuver on the course was believed to be the 60 knot sideward flight capability. Currently, only a few helicopters are actually capable of such a feat. Therefore, with this specific maneuver in mind and with such a high portion of the course being dependent on the rotorcraft's yawing abilities, an auxiliary yaw propulsion system is worth investigating. Several different yaw control systems were then reviewed as potential candidates.

Figure 23. Highlighted portions indicate yawing maneuvers throughout the course

Fenestron

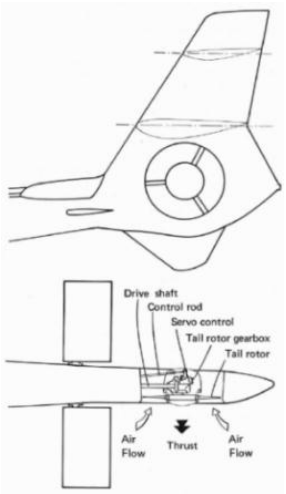

Figure 24. Fenestron

A Fenestron, or "fan-in-fin", consists of a shrouded tail rotor. The ducted propeller creates a more efficient, safer, and less vibrational anti-torque system. In sideward flight, the duct allows more air to pass through the vertical fin which reduces the drag and increases the performance. In forward flight, since the rotor is housed inside the stabilizer it reduces the helicopter's overall drag in comparison to a conventional tail rotor.

The design of the Fenestron was found to have two fundamental "flaws" which makes it unusable for an intermeshing helicopter. First, looking at the design of a Fenestron, seen in Figure 24, the fan can only produce thrust in one direction efficiently. Although the rotor uses a variable pitch system, as thrust is directed in the opposite direction it will interfere with the structural housing and lose thrust. One sided directional control is only half as useful and not worth the system's added weight.

The second design problem is even more intuitive. Synchropters are neutrally stable systems, making a constant anti-torque force unnecessary. The Fenestron would then need to be turned on and off depending on which section of the course the pilot was flying. This greatly decreases the propulsive efficiency and usability of the system. Unless the Fenestron was powered by an instant torque device, such as an electric motor, the constantly turning on and off the motor would be very taxing on the transmission system and the engine. Not to mention the additional amount of time it takes the system to fully wind up/down would negate the benefits of adding an auxiliary yaw unit. Additionally, as found in one of the trade studies, electric motors are also not a feasible option due to the added weight of the batteries.

NOTAR

NOTAR, which stands for a "no tail rotor", is a revolutionary concept patented by McDonald Douglass Helicopters. It uses circulation control to produce lift/anti-torque forces. A simple explanation of how it works is illustrated in Figure 26. However, as previously mentioned, an anti-torque force is not necessary for the Badger's configuration. The main point of interest in the NOTAR system is the rotating directional jet thruster located at the end of the tail boom. This would remove the problem of a one-sided thrust system. The rotating drum could even farther be augmented by creating an auxiliary unit similar to the Aerotécnica AC-14, seen in Figure 25, which provides forward thrust along with directional thrust. Such a design would never require a variable speed transmission since the auxiliary unit could be used in all sections of the course. However, directing the air produced from a fan inside a long tube does not create as much thrust as a regular tail rotor. A simple example is comparing the VTOL British Harrier which redirects its own exhaust to produce lift to the F-35 which uses a lift fan to create the vertical thrust. The F-35 is a much more powerful and efficient system. But, as long as the helicopter does not need a more powerful auxiliary unit, the NOTAR directed jet thrust system is a potential candidate.

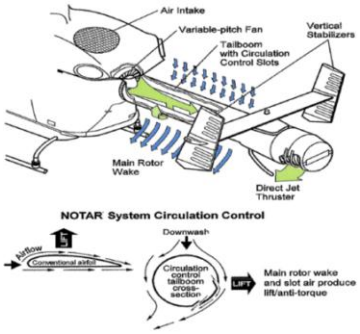

Figure 26. NOTAR System Diagram

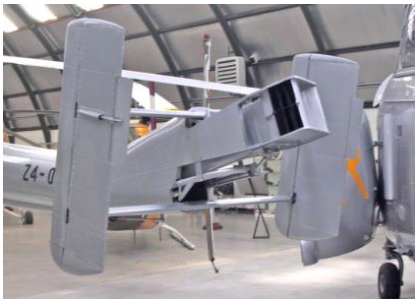

Figure 25. Aerotécnica AC-14 Directed Jet Thruster with Additional Forward Thrust Ability

Swiveling Pusher Propeller

The idea of a swiveling pusher propeller would at first seem to be the best balance of directional control and forward flight speed capabilities. It does not have the NOTAR's disadvantage of weak thrusting abilities or the one-sided Fenestron thrust problem. However, there are clear disadvantages that make this design unfeasible. The device would require very heavy mechanical linkages adding weight and intense mechanical complexity in the swiveling mechanism and in the control system (Engineering, 3-31). Also, it is unclear that the propeller would be able to turn a complete 180°. Without the capability of turning a complete 90° left or right, it would complicate the 60 knot 90° sideward flight maneuver requirement even more. The clear disadvantage of system's complexity and weight, coupled with the very few known positive characteristics, makes this design second to the NOTAR directed jet thruster system.

Intermeshing Main Rotors Only

For steady sideward flight, a helicopter must produce enough thrust in the vertical direction to maintain constant altitude and thrust in the horizontal direction to overcome the flat plate drag. One of the biggest advantages of the intermeshing design is the canted masts that can inherently accomplish both tasks. As the intermeshing helicopter rolls, one hub will produce the majority of the sideward thrust and the other produces the majority of the vertical thrust. The effective sideward flat plate area of the Badger is 41 ft^2 producing 462 lbs of drag as it moves 60 kts sideways at 103° F S.L. Since each rotor produces 1440 lbs of operational thrust, finding the roll angle to achieve steady flight became a simple matter of trigonometry (Figure 27). For the Badger to fly 60 kts sideways, at a gross weight of 2500 lbs the roll angle must be 27°. To fly with the addition of a slung load of 300 lbs and remain at steady level flight, it can only roll 4° and fly at 37 kts. The helicopter will therefore never exceed the 90° bank angle maximum.

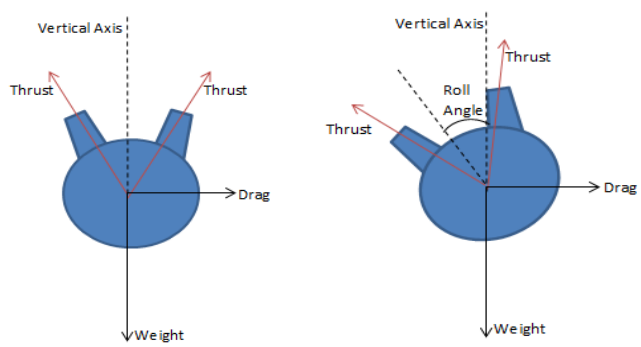

Figure 27. Free body diagrams of the Badger in sideward flight

6.3 Auxiliary Forward Propulsion

After deducing that an auxiliary directional control unit was unnecessary, the next point of interest is an auxiliary forward propulsion system. The Badger's power curve depicted in the performance section shows that the 125 knot at 80% MCP requirement is easily accomplished without any auxiliary propulsion. Therefore, the purpose for adding an auxiliary unit would not be specifically to increase the maximum forward speed, but to increase the longitudinal acceleration and deceleration capabilities. Conventional helicopters with no auxiliary propulsion must pitch down to angle the thrust vector forward as shown in Figure 29. This need for pitching to achieve longitudinal motion is not ideal because it greatly increases the effective flat plate drag, requiring more power to overcome the increased drag. Figure 30 shows the required pitch angle to fly at increasing

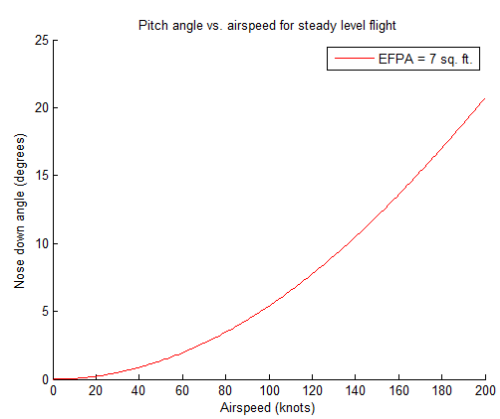

Figure 28. Nose Down Angle Required for Steady, Level Flight vs. Airspeed with no Auxiliary Forward Propulsion

forward flight speeds. The need to pitch also requires more power to overcome the natural tendency of a helicopter main rotor to pitch reward in forward flight caused by the lift produced 90° out of phase on the advancing side of the rotor. This inertial force increases with thrust produced by the main rotor, severely increasing the power required at higher speeds. If a pusher prop was designed to be the main producer of forward thrust, the helicopter would remain level as it accelerates and decelerates increasing the synchropter's agility during maneuvers. The two auxiliary propulsion systems that were then investigated are a ducted fan and a conventional pusher propeller.

Figure 29. Forward Flight Behavior Without Auxiliary Propulsion System

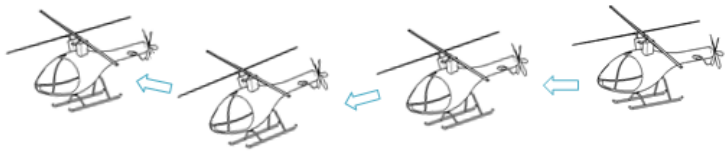

Figure 30. Forward Flight Behavior with Auxiliary Propulsion System

Ducted Fan

A ducted fan is a propeller that has been enclosed within a cylindrical shroud. By shielding the propeller within the duct, it removes the interference between the main rotor wake and the propeller. It will also increase the efficiency of the system by removing the tip vortices which cause a loss in thrust. The primary disadvantage of a ducted propeller is the large increase in drag in both high speed forward flight and sideward flight. This would decrease the maneuverability and agility of the rotorcraft. Another disadvantage is the addition of weight due to the shroud. This adds complexity within the structural system and moves the center of gravity location back even farther, creating instabilities in control. Although the shroud can provide a small amount of thrust vectoring, the ducted fan is still considered unsuitable for this project.

Propeller

A conventional propeller is much more appropriate for the needs of the helicopter's mission. It is a more efficient solution for generating large thrust at moderate forward speeds. Since noise is not a design constraint and along with increased ground crew safety, the main disadvantages of a non-shrouded propeller can be minimized. Thrust modulation can be achieved through a variable pitch propeller and also through varying propeller speed. This configuration would substantially increase longitudinal acceleration and deceleration without adding any unwanted torque in hover conditions. Another design of a non-shrouded propeller is a contra-rotating system. This configuration reduces the swirl velocity in the helicopters wake improving the propeller efficiency and is also a torque free system. However, the complexity of a contra-rotating propeller is very high, and the torque free characteristic is unnecessary once the helicopter is at a moderate speed. A conventional propeller is a far more practical solution for the rotorcraft's mission. In practice, the propulsive efficiency typically peaks at a level of around 0.8 for a propeller before various aerodynamic effects act to decay its performance as will be shown in the following section.

6.4 Pusher Propeller Sizing

The propeller is a variable speed and variable pitch propulsive unit. Through the use of a control mixing, the propeller does not turn on until the pilot has a reached the speed at minimum power. This is because

the propeller isn't required for hovering and low speed maneuvers. After the Badger reaches that speed it will maintain a steady rotational speed. By including creating a variable pitch propeller, the auxiliary unit produces even greater acceleration and deceleration performance.

The propeller was sized using a program called JavaProp, a subprogram of the public and widely used M-H Aerotools website created by Dr. Martin Hepperle. The program uses blade element theory to analyze a single "virtual" blade divided into small sections and handles each section independently from one another. The code will output the best twist and taper for a specified design thrust, tip speed, number of blades, and diameter. The auxiliary propeller for the Badger was designed to produce a thrust that would counteract 80% of the drag in forward speeds, thereby removing 80% of the Badger's parasite power. The design that had the best propulsion efficiency and minimum powered required, at 170 kts maximum forward flight, was chosen in the end. Several trade studies were conducted to see how the tip speed, chord length, and the amount of blades affected different parameters. The final blade geometry is illustrated below:

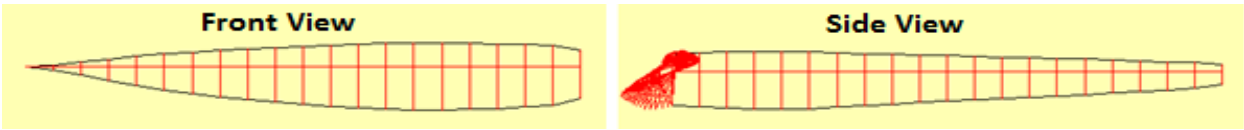

Figure 31. Geometry of final propeller blade selection

Tip Speed

Much like a main rotor blade, a high tip speed is favorable for the Badger's auxiliary unit. As tip speed increases, the efficiency increases and power required decreases. From historical trends, most propellers incorporate tips speeds ranging from 650-750. However, with a high tip speed, the problem of Mach divergence arises and more torque would be produced creating an adverse roll moment to the helicopter. Therefore a limit was placed for a maximum tip speed of 722 ft/s.

Blade Number

As the amount of blades increase, the power required and diameter decreases as shown in the graphs from Figure 32. Both results reflect positively in the design process. Therefore a 6 bladed propeller is ideal for designing the auxiliary unit. A limit of 6 blades was created to decrease the amount of blade weight and added complexity. Contra-rotating systems was also deemed inappropriate because of the added system weight pushing the c.g. location even farther back and transmission complexity required to incorporate 4 rotor disks into one single helicopter. As briefly mentioned in the section before, there is a high amount of torque produced with a single propeller system. In order to account for this, the Badger was designed with a one-sided horizontal stabilizer, or asymmetric wing, to counteract any torque produced by the auxiliary propeller. This will be discussed in a later section.

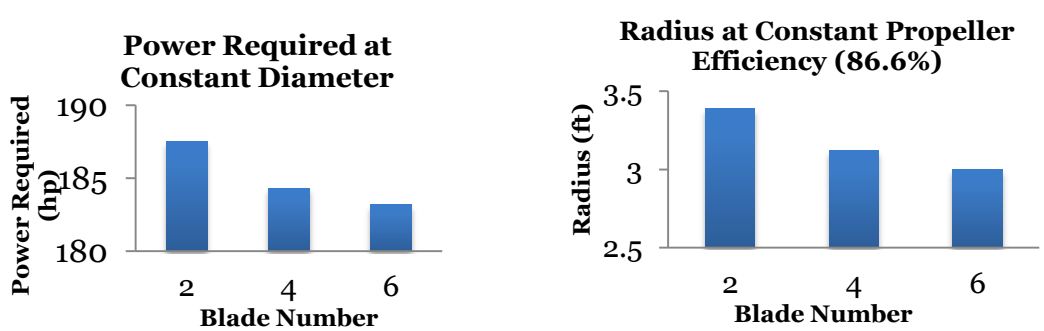

Figure 32. Effects of blade number on the power required and the blades radius

Georgia Tech Rotorcraft Center of Excelence

Airfoil analysis

The next step was to choose the optimal airfoil. The JavaProp program has a list of airfoils used in current pylon racer airplanes and conventional helicopters. The user has the option to specify what airfoil to use at any radial distance along the blade span. Four airfoil configurations were chosen to investigate. The morphological matrix is shown in Table 18.

Table 18: Morphological matrix of airfoil selection

r/R	Option 1	Option 2	Option 3	Option 4
0	MH126	**MH126**	MH126	MH126
0.333	MH112	**MH112**	MH112	MH112
0.667	MH114	**MH116**	Clark Y	Clark Y
1	Mh116	**MH116**	E 193	MH116

After the JavaProp program analyzed each case, the results of the efficiency and power required were compared. It was seen that the efficiencies deviated only slightly while the power required had a much more dramatic shift. From Table 19, the best airfoil configuration is option 2 containing a MH 126 airfoil at the root, MH 112 a third down the span and MH 116 for the rest of the blade.

Table 19: JavaProp results of the four airfoil configurations

Airfoil Configuration	Option 1	Option 2	Option 3	Option 4
Efficiency	80%	**79%**	79%	79%
Power (HP)	194	**181**	208	194

Chord Length

The JavaProp program gives an "ideal" propeller with little to no chord length so it is up to the designer to specify how the optimum chord should be scaled. The end mean chord should be no less than 6 inches. This is the same limit applied to the main rotor disk for structural reasons. A trade study of several scaling and additive factors were applied to the optimum chord and compared against the power required at a range of forward velocities. The best chord scaling factor that had the least amount of power required, while still meeting the 6 inch mean chord minimum, was to add 4 inches to the original chord length. The final propeller dimensions are listed in Table 20.

Table 20: Dimensions of final auxiliary propeller

Radius (ft)	3
Mean Chord (ft)	.425
Blade angle at ¾ chord	28.1°
Number of Blades	6
Solidity	.271
Airfoils	MH 126/MH 112/MH 116
V/nD	1.026
Maximum Thrust (lbs)	511
Power required at 170 kts (hp)	146.4
Efficiency	79%
RPM	2300

6.5 Asymmetric Wing

The Badger incorporates an auxiliary pusher type propeller to increase the acceleration and deceleration performance. Since the 6 bladed propeller is not a contra-rotating configuration, the torque produced will cause the helicopter to become unstable. In efforts to cancel this torque without adding a very heavy and complex system, a single asymmetric wing is added to the design. The wing acts much like a "stand-alone"

aileron. Rotated by a mechanical linkage, the entire surface will pitch 0°-12° to produce a roll moment equivalent to the propeller's torque.

In order to design the wing, it was assumed to have an elliptical lift distribution such that the lifting force would be concentrated at the middle of the wing's span. Therefore, it would need a surface large enough to produce a counter roll moment of 334 lbs-ft (torque at maximum speed) at 12° of deflection. The wing would be designed with the widely used NACA 0012 airfoil which has a stalling angle of 16° (Theory). A limit of 12° of deflection was chosen to account for the slight pitching up motion from the helicopter as it decelerates from maximum speed. Figure 33 is a plot of the torque produced by the propeller and the equal and opposite roll moment produced by the asymmetric wing.

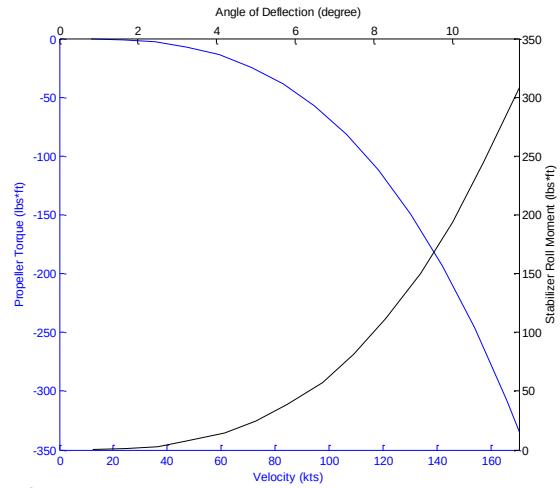

Figure 33. Plot of torque produced by propeller and the counter roll moment produced by the asymmetric wing

Another important factor of the asymmetric wing is the location. If the control surface is placed too far back, the pitching moment created would make the helicopter unstable. Also, since the rotors are canted at 13° and has a flapping angle of 13° with 1° of pre-cone, the wing must be placed where blade cannot strike it. Luckily, if the asymmetric wing was placed at the center of gravity (no pitching moment produced), there will be 2.52" of clearance from the rotor blade at maximum flapping angle to the tip of the asymmetric wing. An illustration of this distance can be found in Figure 34. The final dimensions and location of the asymmetric wing are listed in Table 20.

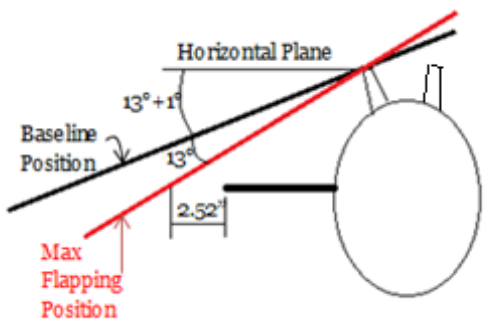

Figure 34: Illustration of rotor clearance. Not to scale

Table 21: Dimensions and location of the asymmetric wing

Span (ft)	2.8
Chord (ft)	0.8
$C_{l_{\delta_{horizontal\ stabilizer}}}$	0.19
Waterline (ft)	3.9
Buttline (ft)	0
Stationline (ft)	13

7 TRANSMISSION

The transmission for the GT-Badger is a 3-stage transmission from the engine to the main rotors as well as a single stage from the engine to the auxiliary propulsion. Several different designs were considered as the transmission was implemented into the CATIA model. The first design was a two-stage transmission consisting of two bevel gears with the same gear ratios as the last two stages shown in Table 22. When the engine and transmission were placed into the 3-D model, it was found that one more stage was needed. In addition when it was decided that our helicopter needed an auxiliary propulsion unit, an additional stage was added to reduce the RPMs from the engine to the rotor. A clutch box

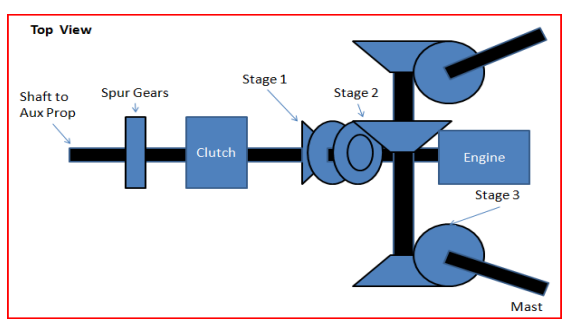

Figure 35. Top view schematic of transmission

Georgia Tech Rotorcraft Center of Excelence

for engaging the propeller was added. Figure 35 is a schematic of the final configuration. Note that the three stage pinions and gears shown are all bevel gears.

The individual gears were sized using equations found in Robert L. Norton's *Machine Design: An Integrated Approach* 3rd Edition. The goal in sizing was to reduce the RPMs from 6000 (an approximate engine speed) to 516 RPMs (the rotor speeds). The overall gear ratio required to do this is 11.63. The overall goal of the design was to size minimal gears that would not add too much weight. The weight was approximated as the volume of a cylinder times the density of the material chosen (VASCO X2M). The optimal configuration that minimizes the weight is shown in Table 22. It was found that making the last stage of the main configuration have the highest gear ratio greatly reduced the weight of the transmission because it reduced the amount of torque placed on both the pinion and the gear. This in turn reduced the weight of the third stage, the main contributor to the overall gear weight. The overall optimized weight of this transmission configuration for the engine sizing is given in the weight breakdown section.

Table 22: Gear Sizing

	Stage 1: 1		Stage 2: 2.9		Stage 3: 4		Aux Spur: 2.6	
	Pinion	Gear	Pinion	Gear	Pinion	Gear	Pinion	Gear
Diameter (in)	5.68	5.68	4.00	11.63	3.75	15.00	3.00	7.83
Face Width (in)	1.50	1.50	1.80	1.80	2.20	2.20	0.85	0.85
Teeth	25	25	20	58	15	60	15	39

8 AIRFRAME DESIGN

8.1 Material Selection

Several trade studies were conducted with respect to material decisions. The primary objective was to effectively choose technologically advanced materials and manufacturing methods that would result in weight reduction while keeping in mind the aircraft's structural integrity, pilot safety and cost effectiveness. Ultimately, concluding educated decisions were made and a component-material breakdown was constructed.

- The airframe is to be constructed of a mixture of graphite – epoxy composites for the case of the bulkheads and Aluminum alloys for the rest of the body. This allows for a high strength, low weight, and durable airframe for best weight reduction to cost ratio.
- To avoid excessive costs of designing complexly curved composites, structural supports in the cockpit are monocoque structures; therefore, these do not have an outer composite skin.
- The fuselage skin of the aircraft is constructed of high strength, lightweight fiberglass.
- The cockpit windows are constructed from acrylic glass for its strength and durability.
- The cockpit door is made of acrylic glass with fiberglass frame and is attached to a steel hinge.
- Flooring areas will be composed of impact absorbent materials in order to increase the safety.
- Main rotor and propeller blades will be comprised fully of composite materials.

8.2 Fuselage Structure

The airframe was designed to be as lightweight as possible while still withstanding maximum aerodynamic loads. The airframe and the internal systems configuration are depicted in Figure 36. In order to maintain static stability while preserving a lightweight airframe, the use of multiple beam types is necessary. The uppermost and bottommost longerons as well as the two rib sections between the bulkheads are I beams. These beams will carry the internal systems and are subjected to the highest loads. The ribs in the tail section are I beams and will carry the supports for the auxiliary propulsion shaft. The

longerons are used as stiffeners to maintain the fuselage shape and provide resistance to any torsion the airframe may encounter. FEA was also performed on the fuselage, confirming a successful design.

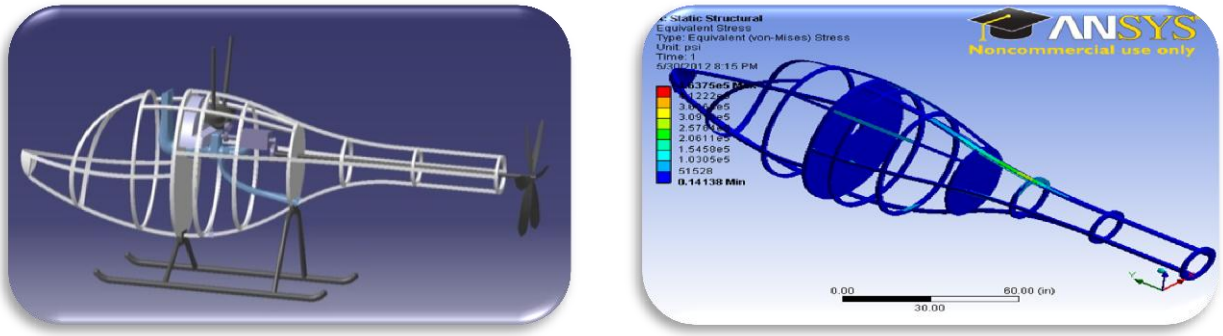

Figure 36: Badger's airframe with engine, fuel tank, and transmission placement

8.3 Landing Gear

The landing gear is composed of hollow aluminum alloy tubes. Dimensions were concluded after several iterations of FEA were performed on the supports (Three inches in diameter and 0.5 inches thick). Using ANSYS static structural toolbox, loads ranging from zero to three G's were applied to the landing gear supports in order to ensure a successful design. As seen in Figure 37 the landing gear is well below the yield stress of the aluminum alloy and therefore satisfies safety requirements given by the RFP.

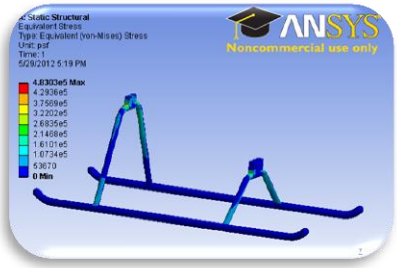

Figure 37. FEA on Landing Gear

8.4 CG Travel

The center-of-gravity (CG) is the point at which an aircraft would balance if it were possible to suspend it at that point. It is the mass center of the aircraft, or the theoretical point at which the entire weight of the aircraft is assumed to be concentrated.[FAA] Its distance from the reference datum is determined by dividing the total moment by the total weight of the aircraft.[FAA] The center-of-gravity point affects the stability of the aircraft. To ensure the aircraft is safe to fly, the center-of-gravity must fall within specified limits established by The BADGER team. Thus, special consideration was taken with the placement of each member. Figure 38 below represents the placement of the center of gravity before and after the fuel has been burned through the race.

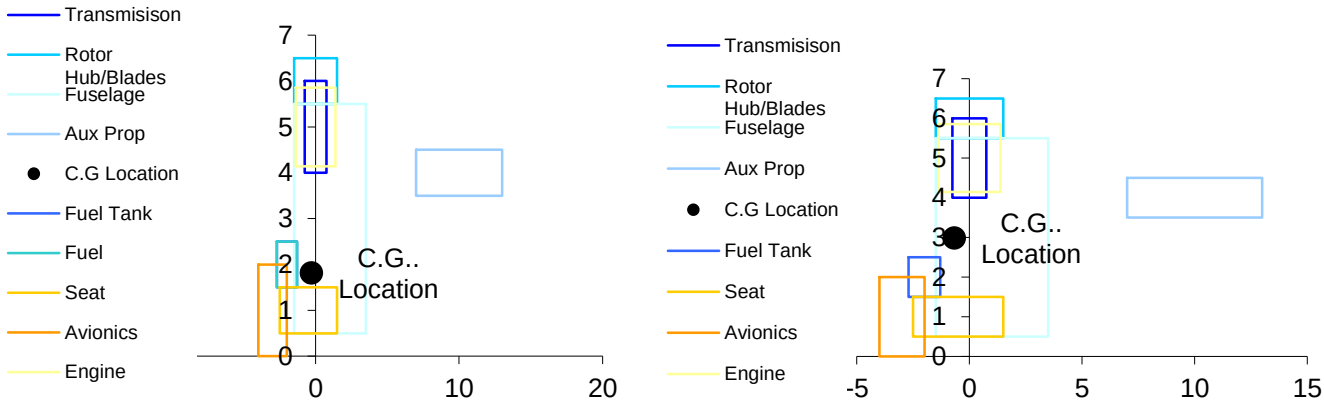

Figure 38. C.G. Travel throughout Race

9 COCKPIT DESIGN

9.1 Visibility

In order to meet the FAA vision requirements described by MIL-STD 850B, the cockpit was designed using the Marenco Swisshelicopter, a high-visibility two-seat concept first introduced in 2011, shown here in Figure 39 The Badger was designed for a single pilot using large window panes similar to that of the Swisshelicopter. The three planes shown in Figure 40 represent the pilot's range of vision at 0, 90, and 135 degrees. Clearly, all vertical and horizontal visibility requirements are easily met with the use of this design.

Figure 39 Marenco Swisshelicoper

Table 23: Minimum Requirements by MIL STD 850B

Minimum angles of unimpaired vision available to the pilot from design eye position	
0" azimuth	At least 25°down and 70° up
20" azimuth	Left and right, 25° down and 70° up
30" azimuth	Left and right, 30° down and 70° up
90" azimuth	Left and right, 50° down and 70° up
135" azimuth	Left and right, 34° down and 70° up

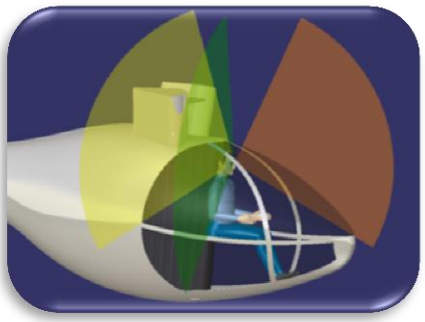

Figure 40. Badger Visibility with compliance to RFP Requirements

Figure 41. Inside View of Cockpit

Most modern aircraft have switched over from the traditional style of analog dials and gauges to the more advanced "glass cockpit" concept. The glass cockpit features electronic (digital) instrument displays, typically large LCD screens, and flight management systems. These flight management systems can be used to display pertinent information as needed, without cluttering the pilot's vision with all the aspects of the flight data at every given moment. The sensors used to feed these systems have also been innovated. Newer designs implement Attitude and Heading Reference Systems (AHRS) as opposed to traditional gyroscopic flight instruments. In order to comply with requirements given by RFP, an inside view of The BADGER's cockpit has been provided.

9.2 Avionics

The Badger cockpit is implemented with an Electronic Flight Instrumentation System (EFIS) in a 7" Dynon Skyview Display panel, shown here in Figure 42. It is an uncertified, low cost avionics option, suitable for the Badger since it is an experimental aircraft and does not require expensive certified instrumentation systems. The Skyview contains a Primary Flight Display system (PFD), a moving map, and engine monitoring system. The PFD provides pertinent flight data, such as roll, pitch, and yaw attitudes, as well as airspeed and heading. The moving map contains all of the navigation information, including a pre-installed layout of the pylon course. An Engine Indication and Crew Alerting System (EICAS) is also programmed into the suite which will alert the pilot with a repetitive beeping if there is a problem or a certain condition isn't being satisfied. For the pylon course, in

Figure 42. Skyview Display

addition to standard engine failure alerts, it will also be programmed to alert the pilot when his altitude reading is too close to the penalty zone at 200 feet. Also, since there is only a 10 minute warm up limit and only 5 minutes allowed for take-off, the display will contain an automated checklist for the pilot to use. This removes the need for a paper manual and extremely convenient for the pilot.

The cockpit also incorporates a heads-up-display (HUD) that projects the optimal course trajectory onto the helicopter's windshield. The HUD provides a transparent virtual overlay of the optimized course along with key flight performance data such as altitude, airspeed, a horizontal line, heading, turn/bank/pitch angle. By letting the pilot to view the optimal route, it reduces their workload and provides them with a choice of which trajectory to follow. The HUD allows the pilot to view vital information without looking away from their usual viewpoints.

An additional switch is added to the suite in order to control the cargo hook. The Badger is installed with an AS29-05-02 support cargo hook by Indraero Siren, shown in Figure 43. While most cargo hooks are designed for very heavy loads, usually a few thousand pounds, this lightweight model has a max capacity of 600 pounds, making it the perfect choice for the 300lb slung load capability requirement. The hook contains a quick release pin, connected to the switch in the cockpit, in case of a structural or safety emergency.

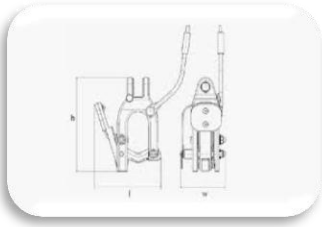

Figure 43. Cargo Hook

9.3 Pilot Cueing System and Envelope Protection

The Badger utilizes a soft stop pilot cueing system on the collective lever, cyclic control stick, and the foot pedals. As the pilot nears the operational flight envelope of the helicopter, the controls exhibit a resistance to further pilot input. These soft stop points allows for safe operation and reliability of the synchropter. Should the pilot require further input for an emergency situation, the controls will continue to operate past the soft stop point with a larger application of force to push or pull on the controls. The soft stop system is more intuitive and natural for a pilot than indicator lights on a dashboard. In the strenuous environment of pulling high G maneuvers in a helicopter, providing the least number of distractions to the pilot as possible will help the pilot focus on the race.

10 FLIGHT CONTROL SYSTEM

The problem posed by the AHS for this competition is unique in that the desired characteristics are based on quickness and speed instead of range or carrying capacity. This required a special analysis of the helicopter's performance necessitating a flight dynamics model to simulate the helicopters response with relative accuracy. The modeling and simulation effort is performed using Heli-Dyne+ (Ilkay Yavrucuk1, 2010), a program developed by Dr. Ilkay Yavrucuk and his students of the Middle East Technical University.

10.1 Modeling and Simulation

The intermeshing configuration was modeled in Heli-Dyne+ as a conventional single main rotor helicopter configuration with no tail rotor, combined with a separate main rotor, each with appropriate shaft tilt angles. The rotor models used Blade Element Momentum Theory and flapping dynamics. The fuselage is a point mass with an associated flat plate drag area to account for aerodynamics. After the model was build, it was exported into the Simulink environment. The auxiliary thrust was added to create the complete synchropter model in Simulink. The auxiliary power is also modeled using Momentum Theory by including a thrust force just enough to account for about 80% of the parasite power and the corresponding torque, which contributes as a rolling moment to the model. As a result, the thrust generated from the auxiliary thruster is scheduled with the vehicle's flight velocity.

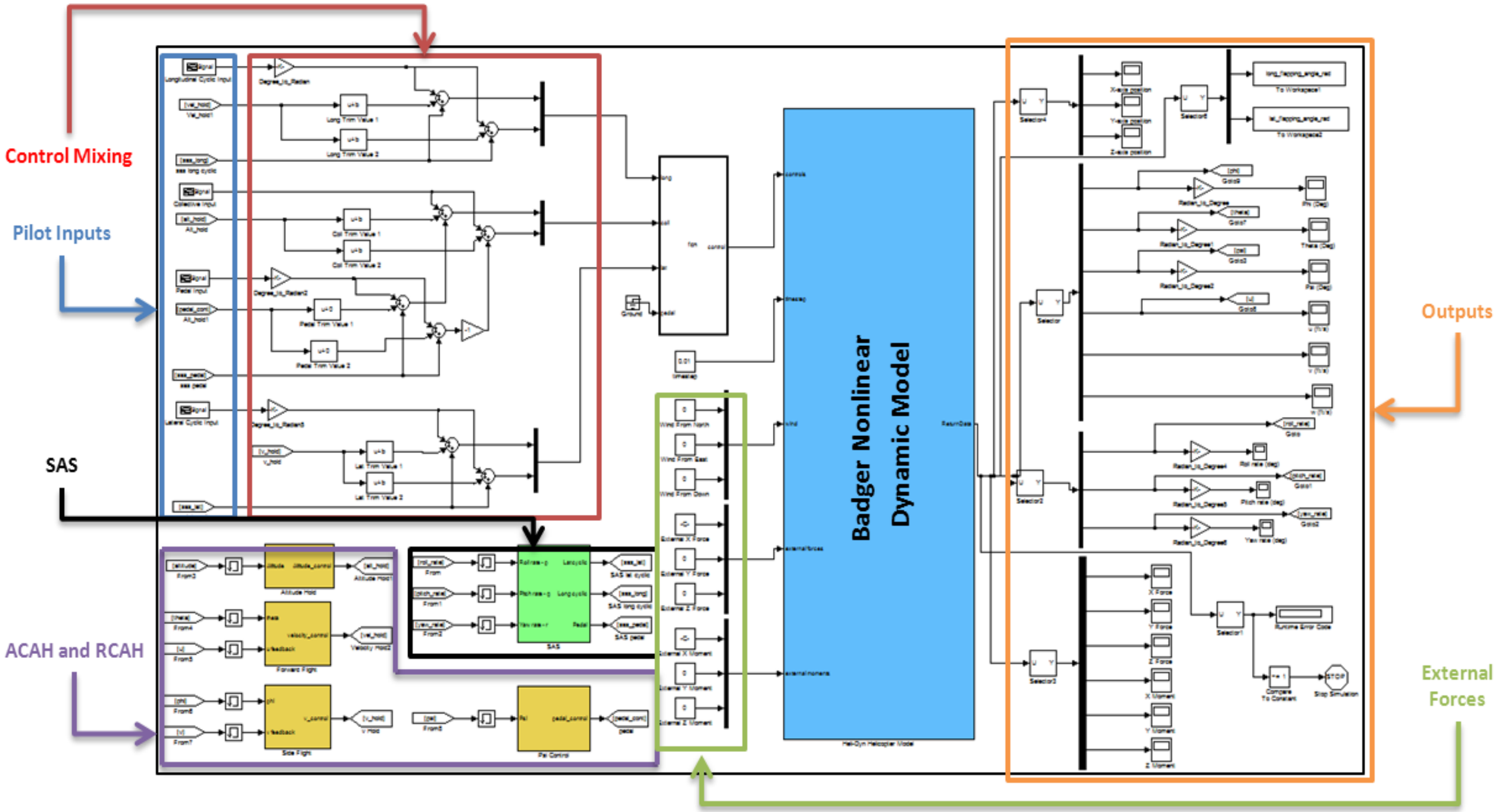

Figure 44. SIMULINK Non-linear Flight Dynamics Model Constructed from Heli-Dyne+

10.2 Control Mixing

A control mixing algorithm was then added to the model. The pilot uses the classic pilot controls (δ), i.e. collective, longitudinal cyclic, lateral cyclic, pedal in the cockpit. Mixing is seamlessly handled in the control system. Since the two rotors are symmetric, the collective, longitudinal and lateral cyclic inputs are equally distributed to each rotor. The pedal control inputs are subtracted from the collective servo tab control of one rotor and are added to the collective control of the other, while also inducing slight longitudinal cyclic inputs on each rotor in opposite directions for a faster yaw response. As a result, the difference in torque of each rotor ,as well as the moments of the tilted force-couple, create a yawing moment.

10.3 Controller Design

The Badger aircraft features a SAS, an Attitude Command Attitude Hold (ACAH), a Rate Command Attitude Hold (RCAH) system, and velocity hold and altitude hold mode controllers. The ACAH is designed for precise maneuverability in low speeds and the RCAH is designed for high speed maneuvering for improved agility. All controllers are linear PID controllers with command filtering. The switch occurs automatic after 50 knots forward flight, however, can be turned on and off through a switch on the collective control. The SAS is active throughout the flight envelope. The velocity hold, altitude hold modes are activated by knobs on the fly-by wire active control sticks. Similarly the auxiliary thruster automatically provides thrust scheduled with the instantaneous forward velocity. The scheduling is based on the required thrust to overcome about 75% of the calculated parasite power. All control loops were designed using Matlab /Simulink. A block diagram of the final system is given in Figure 45

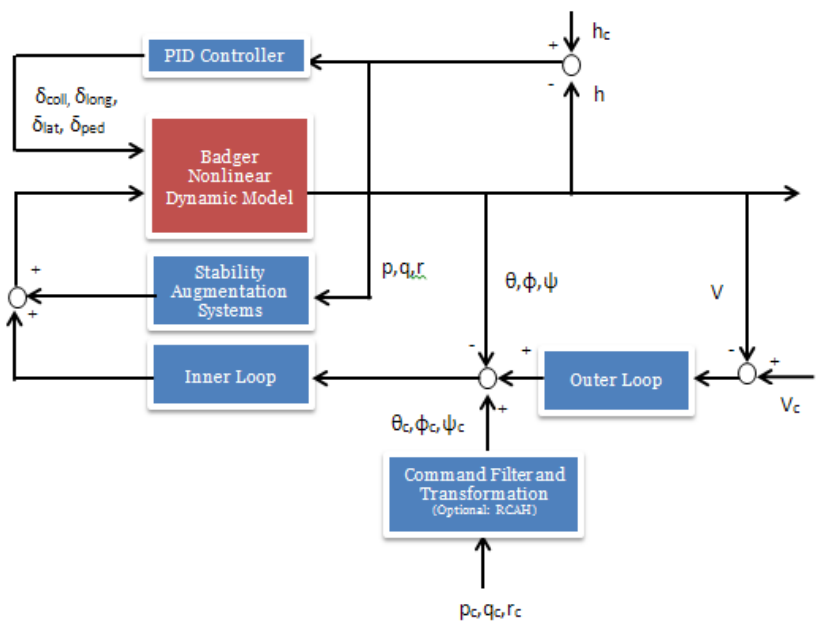

Figure 45. Controller block diagram

SAS, ACAH, RCAH Control Systems

A Stability Augmentation Systems (SAS) are necessary to achieve Level 1 handling qualities throughout the flight envelope. As it was not possible to linearize the highly nonlinear model in Simulink, gain tuning was used to achieve match Level 1 Handling qualities. Roll, pitch and yaw rates were fed back to linear PID controllers in each channel to the lateral cyclic, longitudinal cyclic and pedal actuator controls, respectively. Table 24 below shows the PID gains used in The BADGER's SAS.

Table 24: PID Gains

	Roll Gains			*Pitch Gains*			*Yaw Gains*		
Forward Velocity (knots)	**Kp_p**	**Kd_p**	**Ki_p**	**Kp_q**	**Kd_q**	**Ki_q**	**Kp_r**	**Kd_r**	**Ki_r**
0	0,4	0,3	-0,1	-4	-1	1	1	0	0,008
80	1,4	0,1	0,2	-2,8	-0,5	0,12	1	0	0,008

In addition, a control system is designed around the SAS to achieve ACAH and RCAH controls for the pilot. The inner loop of Figure 45 is an attitude controller which can use either the Euler Angles, or the body angular rates as commands. As a result, the same gain scheduled controller can achieve an ACAH system when Euler angles are used as command inputs or RCAH system when body angular velocities are used as pilot inputs and are converted to Euler angle commands.

Figures 46 and 47 show the augmented response of the aircraft to a step input in the pitch and roll channels, when the aircraft is in hover and the ACAH system is active. Similarly, Figures 48 and 49 show response plots for the aircraft in 80 knots forward flight to step control inputs when the RCAH system is active.

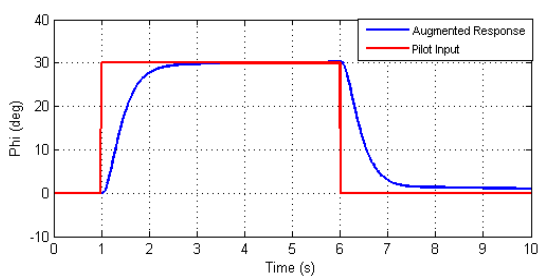

Figure 47. Pilot Roll Input and Augmented Response in Hover using ACAH

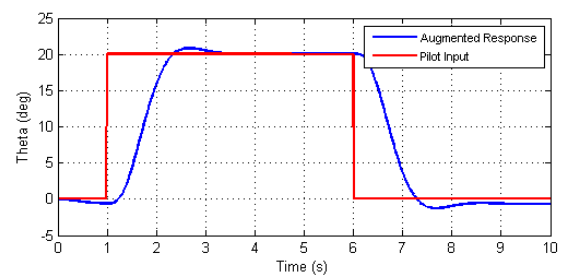

Figure 46. Pilot Pitch Input and Augmented Response in Hover using ACAH

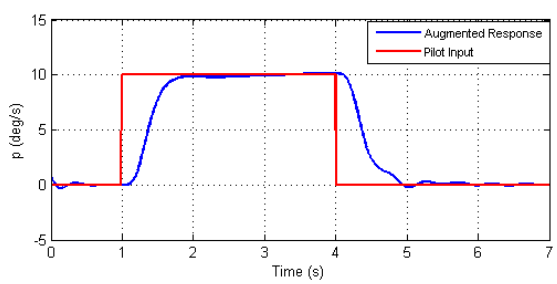

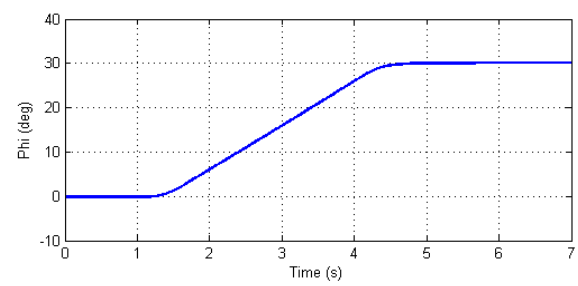

Figure 48. Pilot Roll Step Input, Roll Rate and Roll Angle Response using RCAH at 80 knots

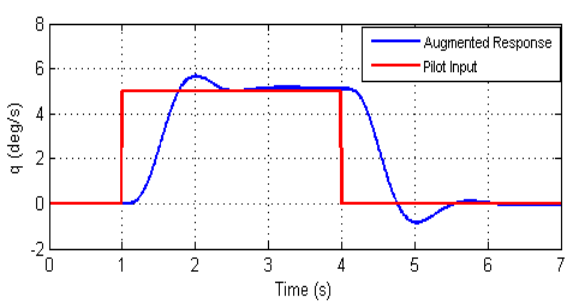

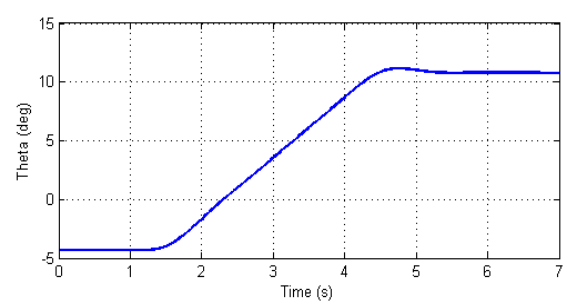

Figure 49. Pilot Pitch Step Input, Pitch Rate and Pitch Angle Response using RCAH at 80 knots

Altitude Hold and Velocity Hold

The outer loop controller generates attitude commands that will allow the aircraft hold or achieve a certain velocity as shown in figure 50. Similarly, a feedback to the collective control allows the Badger to hold altitude. Both controllers were designed using PID controllers and were tuned to reach fast responses. Examples for both forward velocity and side velocity command responses using the combined SAS, inner and outer loop controllers are shown in Figures 51 and 52.

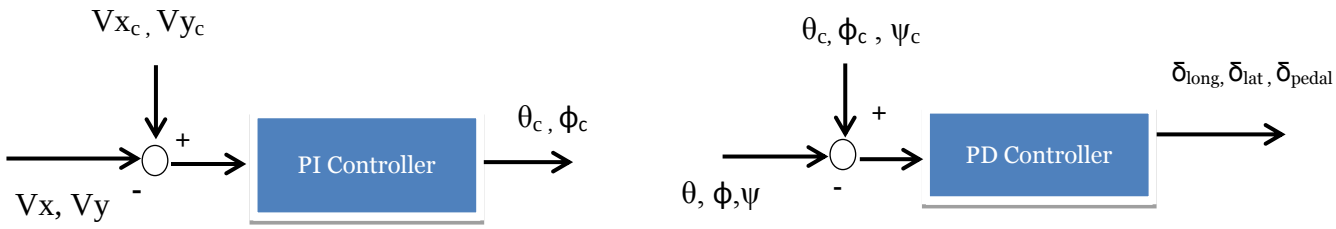

Figure 50. Outer loop (left) and inner loop (right) block diagrams

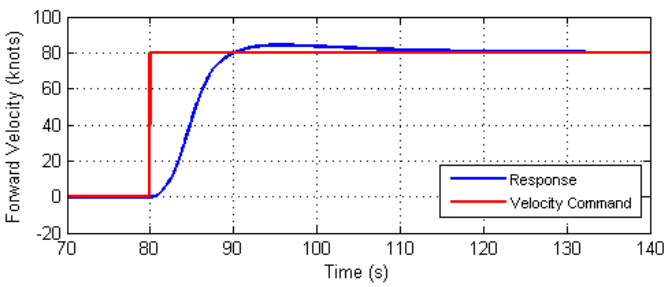

Figure 52 Forward Velocity Command Response

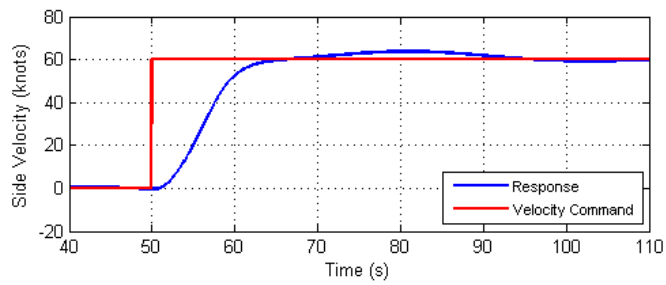

Figure 51 Side Velocity Command Response

10.4 Trimming

Trim solutions are found using the controllers by accelerating the model to the appropriate flight velocity from a hovering flight condition. Results are shown below in Table 25.

Table 25: The trim values and auxiliary propulsion with different forward flight velocities

Initial Conditions at 50 ft				Trim Values						Aux Propulsion	
Forward Velocity (knots)	Theta (deg)	Phi (deg)	Psi (deg)	Lat. Flap Angle (deg)	Long. Flap Angle (deg)	Long. Cyclic (deg)	Collective1 (deg)	Collective2 (deg)	Lateral Cyclic (deg)	Thrust (lb)	Torque (lb*ft)
0	0,000	0,000	0,000	0,000	0,000	0,000	14,867	14,867	0,315	0,000	0,000
40	-1,358	-0,258	0,001	0,296	-0,147	2,829	13,129	13,163	0,296	47,630	-7,726
80	-4,332	-0,123	0,008	0,473	-1,663	7,028	14,094	14,344	0,473	190,521	-61,779
100	-5,864	0,000	0,000	0,657	-3,480	10,187	15,581	16,071	0,656	297,689	-120,659
120	-7,252	0,005	0,000	0,706	-6,153	14,200	17,675	18,932	0,664	428,673	-208,495

For the side flight, Heli-Dyne+ is used again in order to extract a new model with concrete block weighting 300 lbs. Again the controllers were used to find the trim point at a sideward flying condition.

Table 26: The initial conditions and trim values at side flight with the slung load

Initial Conditions at 50 ft						Trim Values			
Side Flight Vel. (knots)	Theta (deg)	Phi (deg)	Psi (deg)	Lat. Flap Angle (deg)	Long. Flap Angle (deg)	Long. Cyclic (deg)	Collective1 (deg)	Collective2 (deg)	Lateral cyclic (deg)
60	0,647	33,195	0,194	-4,820	-0,702	0,702	16,860	20,742	-1,048

10.5 Maneuverability and Agility

The gain tuning of the controllers were based on the Handling Quality reports for Maneuverability and Aility. Special considerations were given for the roll response. The Badger's control system has Level 1 Handling Qualities in the roll axis from a maneuverability point of view. A plot is of the aircraft response is provided in Figure 53.

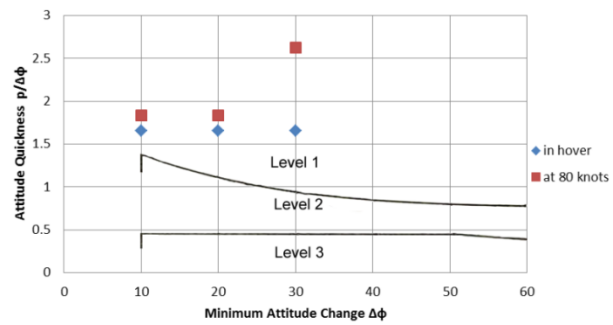

Figure 53. Handling Qualities in the roll axis, (Padfield, 1996)

10.6 Fly-By-Light Architecture

The Badgers control system is a fly-by-light design. This system replaces mechanical linkages with electronic actuators. This control system weighs much less when compared to the heavy fluid, pumps, and linkages of a hydraulic system. The electronic actuators allow for easy implementation of a flight control system computer and have a quick response time which is crucial for a highly maneuverable and agile rotorcraft such as the Badger. The fly-by-light system utilizes light transmission through fiber optic cable which is much less susceptible to electromagnetic interference than fly-by-wire systems.

11 PERFORMANCE ANALYSIS

11.1 Sideward Flight Drag Estimation

Computational fluid dynamics (CFD) was employed to obtain equivalent flat plate area estimates for sideward flight. A simple isotropic fully unstructured mesh was utilized to obtain an equivalent flat plate drag figure of 41 ft². Anisotropic prismatic extrusions to create a boundary layer mesh region employing such concepts as y+ and fitting 20-30 cells in a calculated boundary layer thickness would have been more proper for the analysis, but the use of empirical data validated the CFD calculation. It is hypothesized that this was not as necessary for sideward flight as these methods are intended in large part to predict boundary layer separation, and the separation in sideward is more obvious in that it is more like a flat plate.

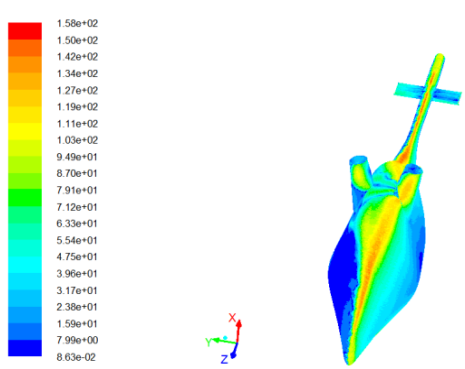

Figure 55. Velocity Color Map for Fuselage in Sideward Flight

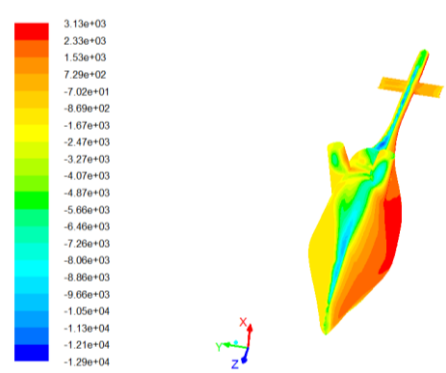

Figure 54. Pressure magnitude color map for fuselage in sideward flight.

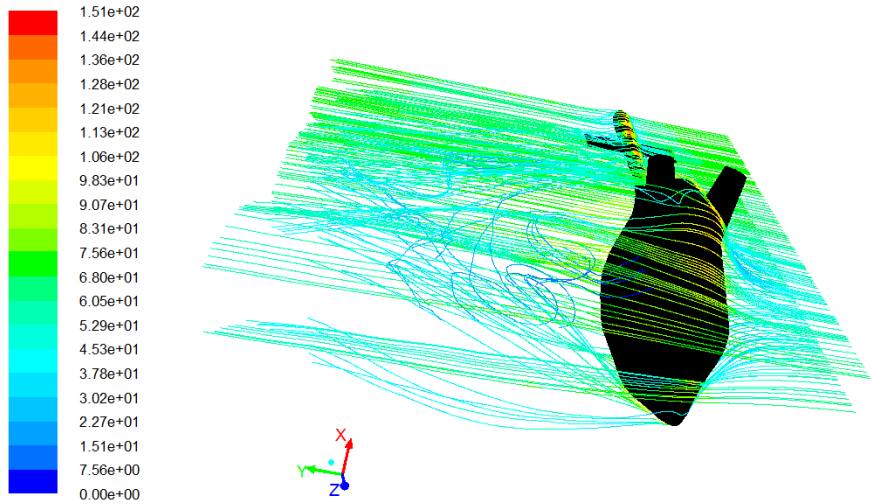

Figure 56. Path lines colored by velocity magnitude (m/s). Freestream velocity is in the positive y direction

The solver employed was ANSYS FLUENT and the mesh generator ICEM. NASA codes such as FUN3D and VGRID were less favorable, even though they were possibly more capable, for the reason that in an international helicopter design effort these would likely not be allowed.

11.2 Forward Flight Drag Estimation

A MATLAB program based on empirical data was used for forward flight drag. A figure of 7.2 sq. ft. was obtained. The inputs to the program are based off of the geometry set by CAD parameters. As expected, the main rotor hub contributes the most to the total drag.

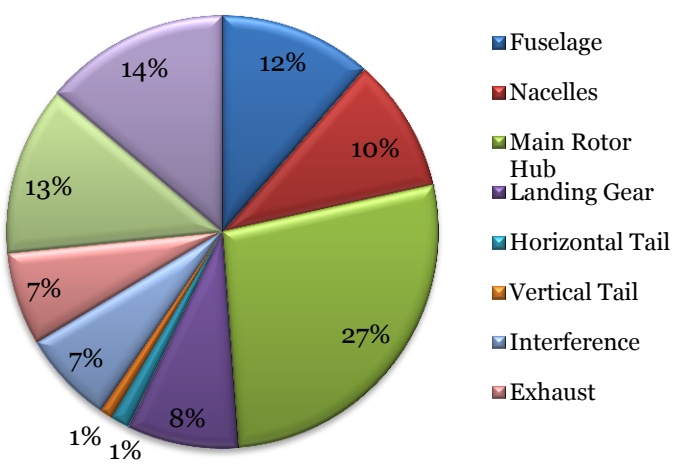

Figure 57. Forward flight drag breakdown

Table 24: Forward Flight Drag Breakdown

Component	Parasite Drag (ft^2)
Fuselage	0.822
Nacelles	0.7263
Main Rotor Hub	1.9638
Landing Gear	0.6
Horizontal Tail	0.101
Vertical Tail	0.07
Interference	0.5
Exhaust	0.5
Auxiliary Propeller	.912
Miscellaneous	1
Total	**7.2**

11.3 The GT - BADGER Calculator

A simple calculator written in Java was developed for synchropter-specific quantities. This calculator was used in the preliminary design phase of the GT-Badger to obtain values such as the projected area of the rotors and other performance parameters such as solidity using the intermeshing areas. A screenshot of the graphical user interface is shown in Figure 58.

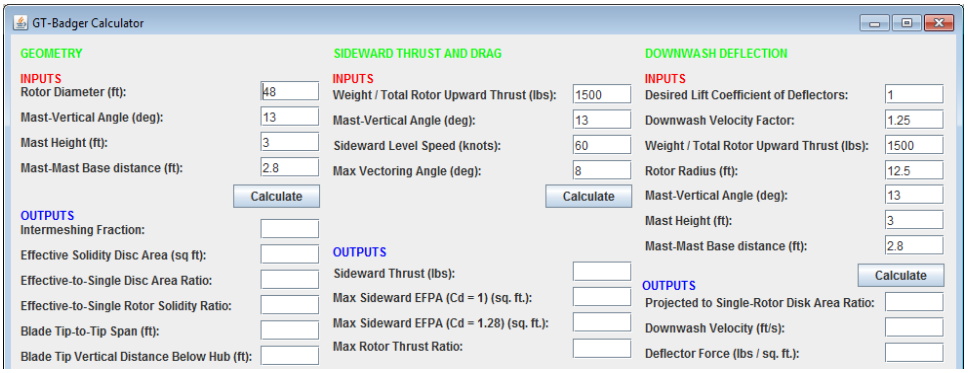

Figure 58. GT-Badger Calculator.

The user interface describes all of the inputs and outputs. Three types of calculators are included. These are related to synchropter geometry, sideward thrust and drag, and downwash deflection. Synchropter geometry calculations were useful in determining adjusted solidity values (since there is partial overlap in synchropters) and ensuring blade tips did not hit the ground or exceed overall width limits. Sideward thrust and drag calculations took into account the cant angle of the synchropter rotor masts. The theoretical capability of the sideward thrust of a synchropter was determined by defining a max vectoring angle, which would be effected by cyclic pitch control. The downwash deflection calculator was to aid in the assessment of an auxiliary yaw control system. This system consists of a number of vertically-oriented flaps at the tail of the rotorcraft in downwash. Adjusting the pitch of these flaps would create a yawing moment due to the interaction of the flaps with the downwash; however, this last concept was not used in the final design.

11.4 Forward Flight Performance

A MATLAB code was developed by The BADGER team based on the roots of momentum theory. A value of K=1.15 was included in the calculation of induced HP to account for tip loss effects as well as a value of Kov = 1.35 to account for the intermeshing fraction between the two rotors. This Value of Kov=1.35 included in the induced power calculation by looking at a tandem rotor configuration and assuming a small angle approximation as shown in Leishman's *Introduction to Helicopter Aerodynamics*. Figure 59 shows a plot indicating how this factor changes as we go from a coaxial state, meaning two rotors placed directly on top of one another, all the way to a state where we find two single main rotors sitting side by sideb.

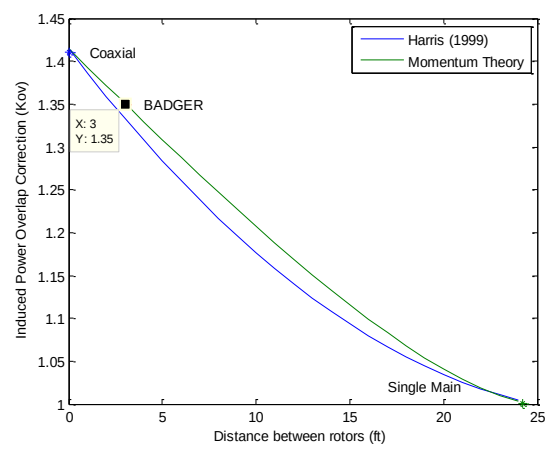

Figure 59. Plot illustrating how the induced power correction factor is a function of mast separation

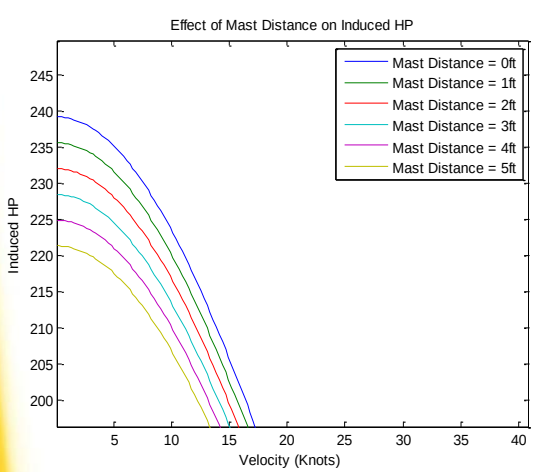

Figure 60. Induced Power as mast distance grows

Another plot of interest that was taken into consideration when sizing The BADGER is shown in Figure 60. In this figure we were able to predict how the induced horsepower was affected by the separation of the two masts. It was only of interest to look at the window between the mast distances of 0 ft to 5 ft since anything greater than 5 ft would not be a desired configuration due to the vehicle size constraints given by the RFP. From this plot we were able to conclude that the separation will have an effect in our induced HP but not considerable enough to make a concluding decision of the separation of the two rotors.

This performance code was calibrated using a blade element momentum theory code developed in class to ensure that its results were accurate and valid. Plots of power available, power required and its components were then plotted to ensure that The BADGER met the performance requirements given in the RFP.

The BADGER was initially sized to meet the requirements given by the RFP without the need for auxiliary propulsion. Therefore, plots showing power required versus velocity were developed and are shown below meeting the requirement to hover at SL 103F as well as the 125 knot cruise flight at 90% MCP.

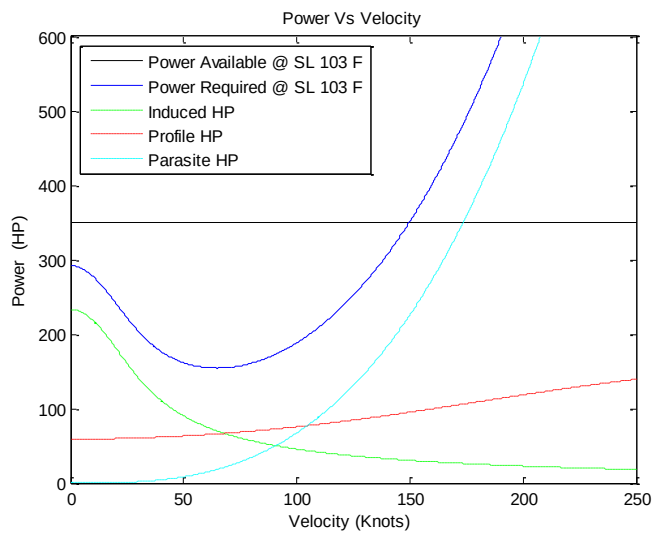

Figure 61. Power Vs. Velocity (No auxiliary propulsion)

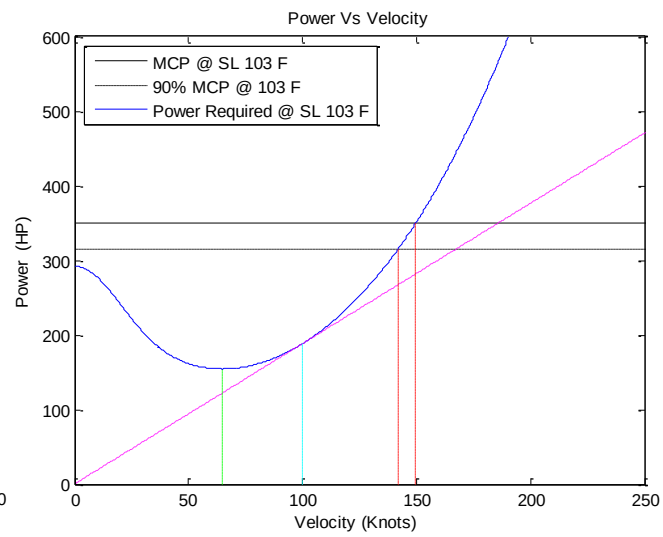

Figure 62. Illustrating the 125 kts requirement at 90% MCP

After the careful review of The BADGER design, the team decided that adding a pusher propeller in order to increase its acceleration and deceleration throughout the race. These reasons are explained above in the pusher propeller section. Analysis developed and shown in Figure 63 led us to conclude that Power required in hover increases drastically with the addition of weight and later converges at higher velocities to a similar maximum velocity. This figure shows how inertial effects make a difference on the Power required curve developed previously. From this curve we concluded that adding a propeller in order to increase our performance would result in an addition of 50 HP to our power available to account for the weight of the propeller and its components.

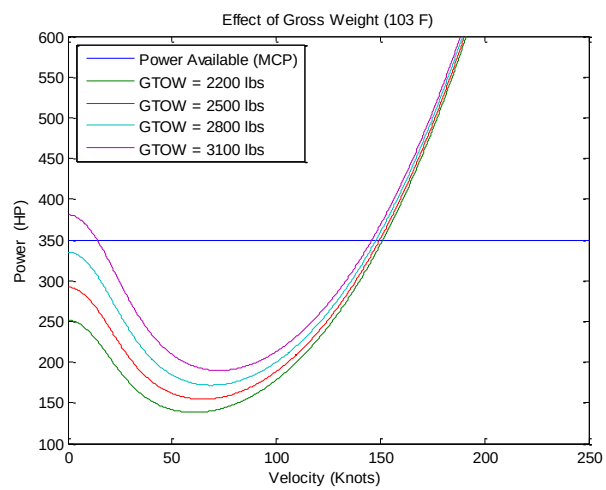

Figure 63. A plot showing how the power required is affected by increased gross weight

The following two plots shown in Figure 64 below represent the new Power Required once the pusher propeller was implemented into the design and the horsepower available was increased to account for the inertial effects encountered previously. The propeller was mathematically represented in a similar fashion as a propeller from a fixed wing aircraft.

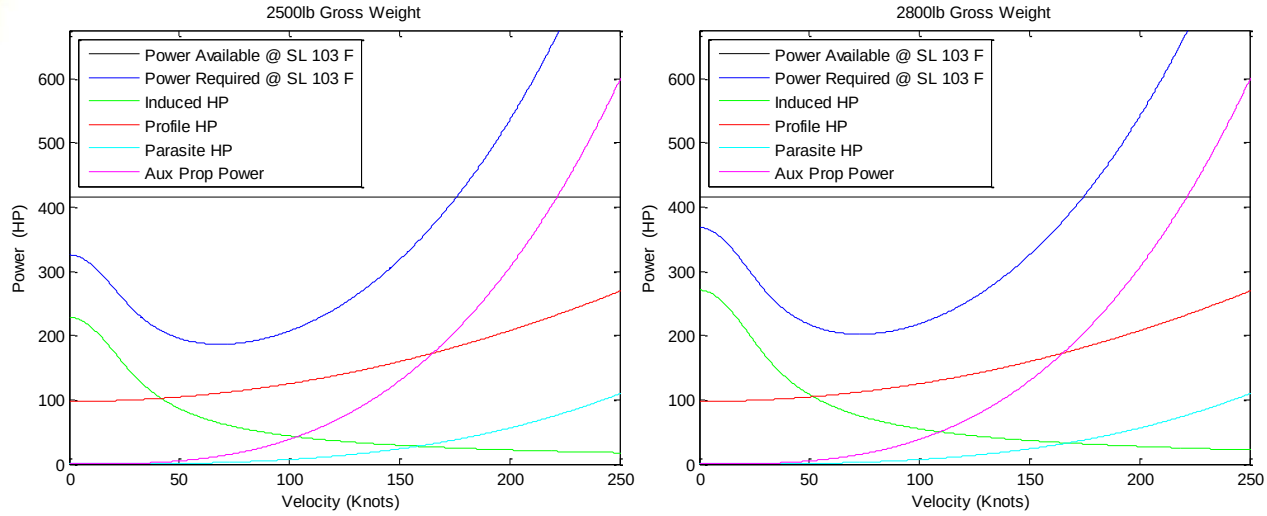

Figure 64. Power Required Curve for both race configurations after addition of a pusher propeller

In order to facilitate the understanding of the previously shown performance curves, plots showing only power available and power required were plotted with the addition of dashed lines going through several points of interest shown in figure 65 below. A horizontal dashed line was included in order to indicate the mark of 90% MCP. This enabled the team to verify that The BADGER in fact did meet two of the requirements given by the RFP. Both plots shown in figure 65 prove that The BADGER does indeed meet the 125 knot cruise speed at 90% MCP at SL 103F, blowing this requirement away by 40 knots in its 2500lb configuration. It was also important to show that The BADGER could hover out of ground effect under the same demanding conditions. It is evident from the two plots below that The BADGER is able to meet its requirements even after a 300lb slung load has been attached in the second section of the race.

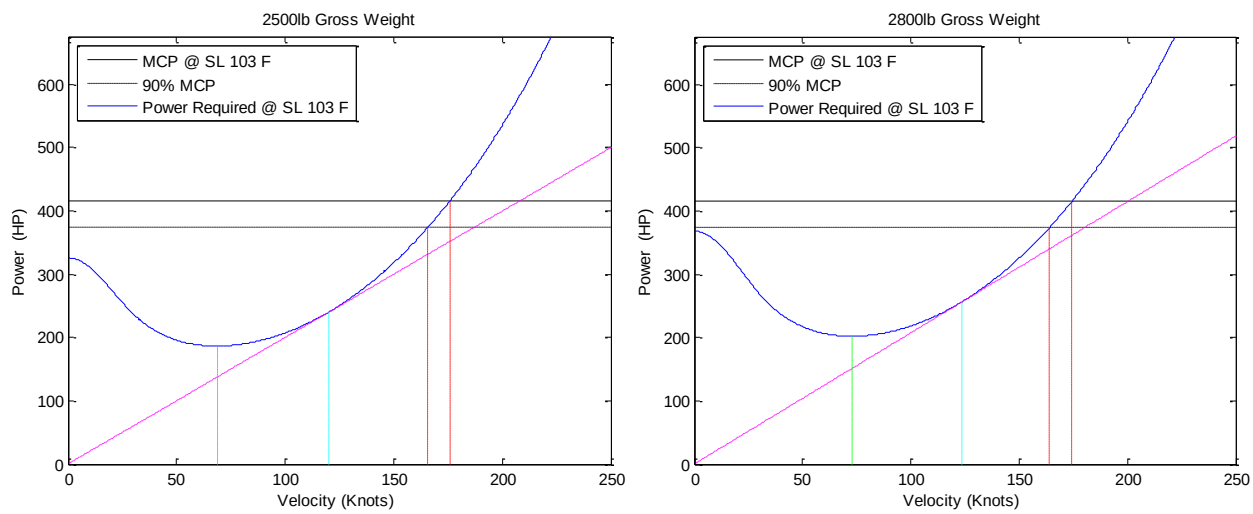

Figure 65. Horsepower v.s. Velocity (knots) with the addition of the pusher propeller meeting requirements given by the RFP

Table 25: Summary of Figure 65 showing values are in compliance with RFP

Parameter (103F)	GW = 2500lbs	GW = 2800lbs
Best range speed	119.8312 knots	123.5676 knots
Best endurance speed	68.5893 knots	73.1264 knots
Maximum speed	175.8769 knots	174.2756 knots
Speed at 90% MCP	165.7353knots	164.134knots

Georgia Tech Rotorcraft Center of Excelence

It is important to understand that The BADGER's performance will in fact be better on the day of the race, as these previous plots assume a temperature of SL 103F in order to prove its performance capabilities and meet the requirements given by the RFP. Since the race will take place in a SL 80F, The BADGER team was interested to see how this aircraft would perform the day of the race. Figure 57, shown to the right, depicts the outstanding performance of The BADGER in beautiful 80 degree F weather on a New York day.

Other performance plots of interest were developed in order to understand The BADGER's capabilities during the race. As one can see from the plots below, a maximum lift to drag ratio average of 4 can be obtained at a velocity of 115 – 130 knot depending on the section of the race and the vehicle configuration.

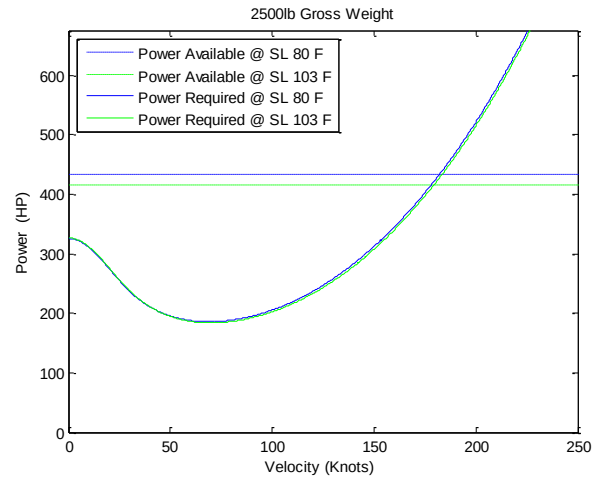

Figure 66. Performance contrast of an 80 deg F vs the required 103 deg F

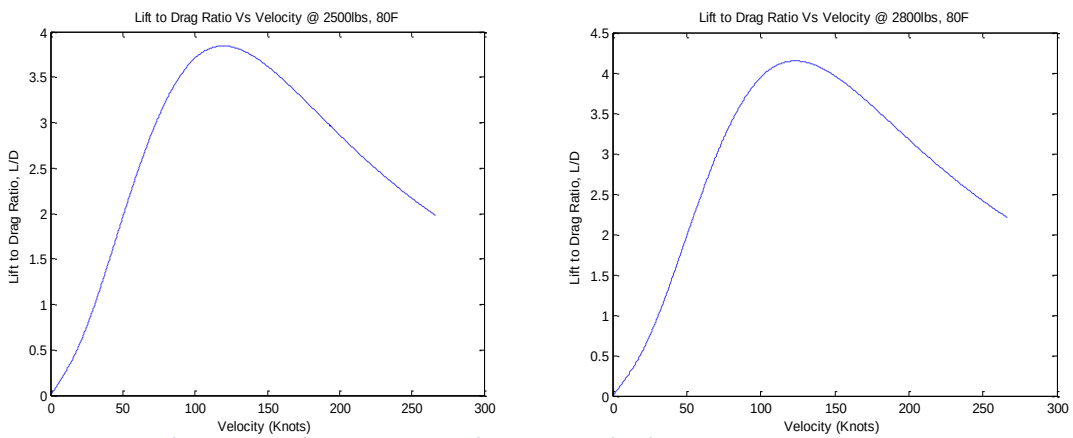

Figure 67. Lift to Drag Ratio Vs Velocity in Knots of The BADGER

Rate of climb of a helicopter is an important performance feature of a helicopter therefore our team decided that it would be a good idea to include this performance parameter in the report. A maximum rate of climb plot vs. velocity was obtained and shown in the figure below where the Y-axis represents the rate of climb with units in (ft/min) and the X-axis represents velocity in Knots.

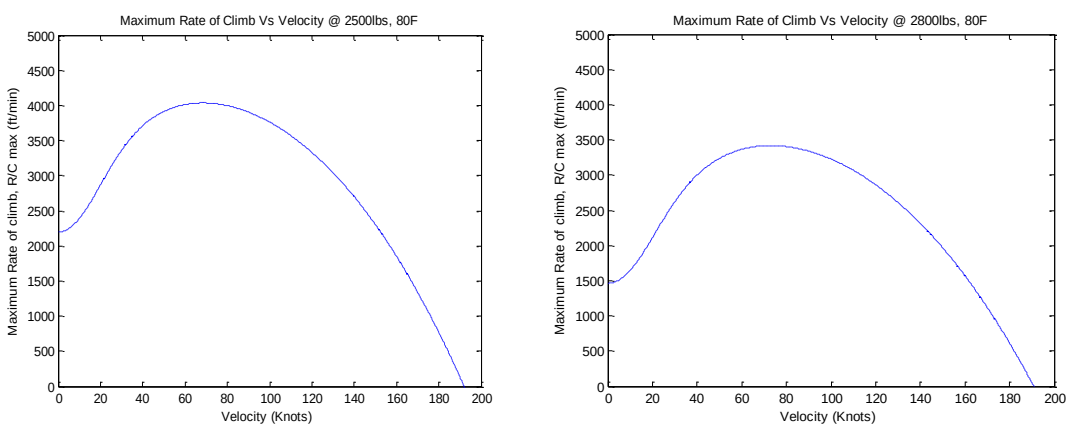

Figure 68. Maximum Rate of Climb (ft/min) Vs. Velocity (knots)

Finally, a plot of minimum turning radius versus velocity was plotted to ensure that our helicopter was capable of performing certain maneuvers expected in the race such as the 300 ft 180 degree turn in the beginning of the track. Using this plot we were able to conclude that this turn should be performed at a velocity that does not exceed 95 knots. The information obtained from this performance section was used while generating the preliminary time calculation performed before a trajectory optimization was performed.

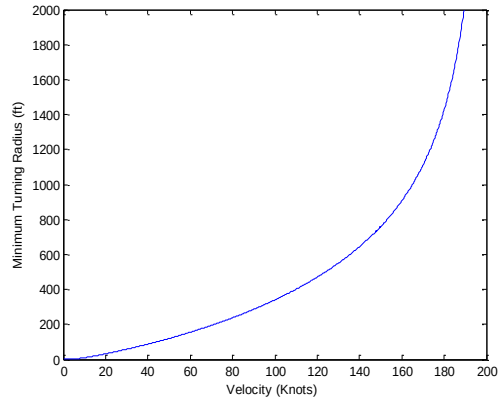

Figure 69. Minimum Turn Radius (ft) vs. Velocity (knots)

12 TRAJECTORY OPTIMIZATION

As per the 2012 student design competition RFP eta function, our vehicle's course completion time must be estimated and minimized as a performance metric. Given that our vehicle is a manned craft being guided by a human pilot through an obstacle course, any calculation of completion time is necessarily an approximation representing what our vehicle can do given realistic control inputs from a pilot.

In an effort to determine how our vehicle would traverse such an obstacle course realistically, we opted to use optimal control theory combined with human-pilot based constraints. By mapping our vehicles progress through the course in this manner, we were able to find the actual control input needed at every step of the course as well as the exact path our vehicle would theoretically fly, thus, showing about how long it would take to complete the course and that the piloting need not be calculated by super-fast computing.

A second reason for this investigation is to have predetermined course path installed into the BADGER's computer and have it projected onto the pilot's helmet visor as a Heads Up Display. This optimal trajectory will serve as a guide for the pilot to follow to achieve the fastest time that is calculated in this study.

12.1 Method

We chose to use GPOPS (General Pseudospectral OPtimal control Software) as our optimal control software because it is open source, contained entirely within MATLAB, and a well-documented, widely used program that our professors had some familiarity with.

We used Heli-Dyne+ to produce linearized state space representations for our helicopter at varying trim conditions, depending on the maneuver in question. Heli-Dyne+ produces the non-linear equations of space as well, but for this task we felt it was sufficient to use linearized models for each maneuver. In order to justify this assumption, we produced linearized models over a range of airspeeds and trim conditions with Heli-Dyne+ and found that within small ranges of state the eigenvalues of our state space matrices held nearly constant. Thus, our linearization assumption should not have produced significant error within the small state range each maneuver contained.

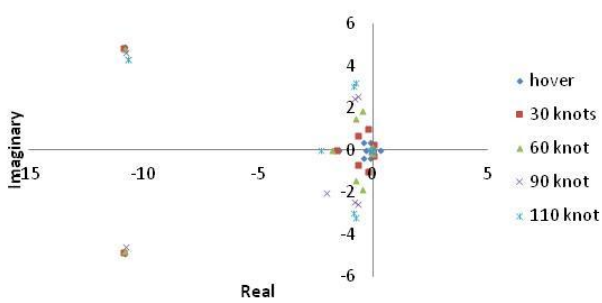

Figure 71. Eigenvalues plotted

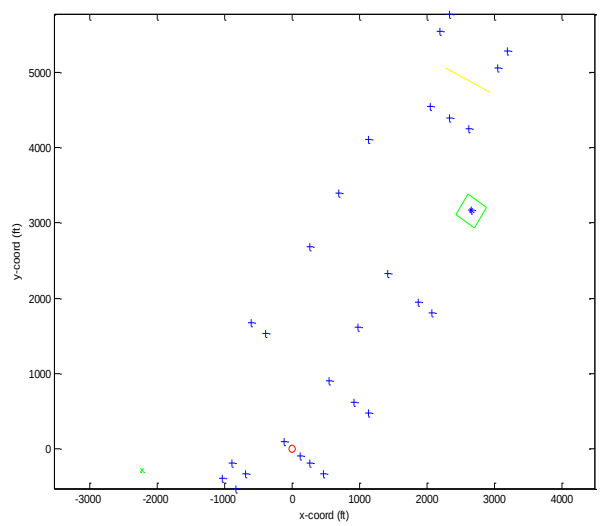

Figure 70. Competition Course Distance Map

Georgia Tech Rotorcraft Center of Excelence

As a bonus, to verify the control inputs produced by GPOPS simulation, we were able to run brief control simulations into Heli-Dyne+ to verify the predicted linear responses were close to the more accurate non-linear ones.

The idea of using optimal control as a means for trajectory optimization is not new, and in fact, several examples exist on the GPOPS website for how to rework the code into an optimal trajectory format. By default, GPOPS simply takes a set of state and control variables, a state-space function relating their time derivatives, and a cost function to minimize, in this case time itself. It is left to the user to define the initial state, the final state, and any constraints/checkpoints in between. For us to create an optimal control simulation, therefore, we had to add states defining earth coordinate system Euler angles and position vectors that could then be tracked and given prescribed beginning and ending values with relation to the course.

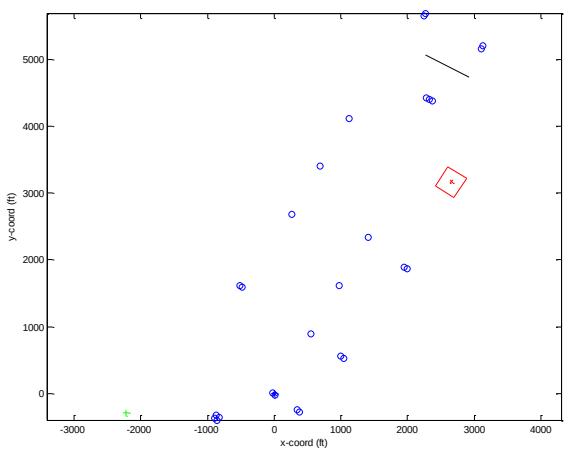

Figure 72. Scaled Course Map

Before tracking our helicopters optimal path through the competition course, we first had to convert the digital map into something more quantifiable and discrete. Using the MATLAB image processing toolbox, a pixel mapping of the course along with the key describing the distance conversion was stored into memory. The distance key was then used to convert pixels into physical distances in feet.

The blue crosses represent pylons, the red circle represents the starting position when time begins, the green diamond represents the landing pad, the yellow line represents the turning limit on the 180 degree turn, and finally the green 'x' represents the completion landing pad. Were this map to scale, the pylons would be hundreds of feet apart, which they are not. The pylons were only shown to be that far apart on the map to better show the course layout. An ad-hoc scaling program was used to bring the pylons 50ft apart. The scaled course map can be seen below in Figure 73.

In the above figure, the pylons are represented by circles, the helipad by a red square, the turn limit by a black line, and the landing pad by a green cross. The helipad is left at large scale because its landing will occur in the center regardless. This more accurate course has the set of coordinates that were used to prescribe constraints and boundaries for the trajectory optimization code. With the scaled map coordinates at hand, we were able to create a set of geographical waypoints for the helicopter to fly through, which were the checkpoint states for the trajectory optimization code.

The course was divided into eleven maneuvers for GPOPS which were the same as those enumerated by the segments 0-9 from the RFP without the staging segment but an added "large radius 180 degree turn" between 6 and 7 and a division between pirouette and pickup. We therefore had eleven linearized matrices and a large number of state waypoints to fly through. The conditions at the beginning and end of each stage were approximated based on trial-and-error along with our best engineering judgment as to what states would provide a happy medium for the best time of two conjoined maneuvers. The waypoints were decided by safety factors such as maximum load factor, pylon clearance, pilot margin of error, and height guidelines. The chosen waypoints can be seen below. Beginnings and ends are always assumed to be at zero lateral speed, vertical speed, roll, yaw, pitch time derivative, roll time derivative, and yaw time derivative. For the sake of brevity, only the aerial 2-D waypoint plot is shown in

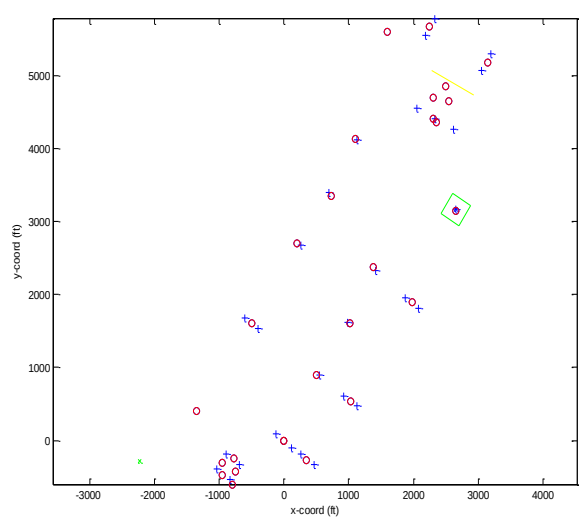

Figure 73. Course Optimal Trajectory Waypoints

Figure 73. The segments' geometric initial conditions are included below as well in Table 26. It is worth noting that the un-scaled pylon positions are used to show the course better as the scaled versions are very close together and do not show up well when seen together.

Table 26: Segment Conditions Table

	Velocity (kts)	θ_{pitch} (rad)	X_{Earth} (ft)	Y_{Earth} (ft)
Start	100	0.2	0	0
Segment 1 End	140	0.4	500	900
Segment 2 End	100	0.15	1375	2375
Segment 3 End	80	0.2	2350	4360
Segment 4 End	60	0.2	1100	4140
Segment 5 End	100	0.4	2250	4725
Segment 6 End	120	0.3	-950	-475
Segment 7 End	60	0.4	-500	-800
Segment 8 End	120	0.3	3125	5175
Segment 9 End	0	0	2650	3150
Segment 10 End	60	0	1975	1890
Segment 11 End	60	0	1025	540
Segment 12 End	150	0.5	350	-275

12.2 Results

From our optimal trajectory code results, we have concluded that our helicopter can feasibly complete the competition course within 4.13 minutes. The plotted courses XY projection can be seen in Figure 74.

The tracking of states for each of the twelve segments, while important to the calculations and verification process, would take an excessive amount of space in this report for what is only one section of the performance evaluation.

Our trajectory optimization method has provided us with a realistic estimation of our completion time while providing the control inputs needed to reproduce this time. We can conclude that our helicopter can complete the course in a range of 4 minutes and 8 seconds with a human operator.

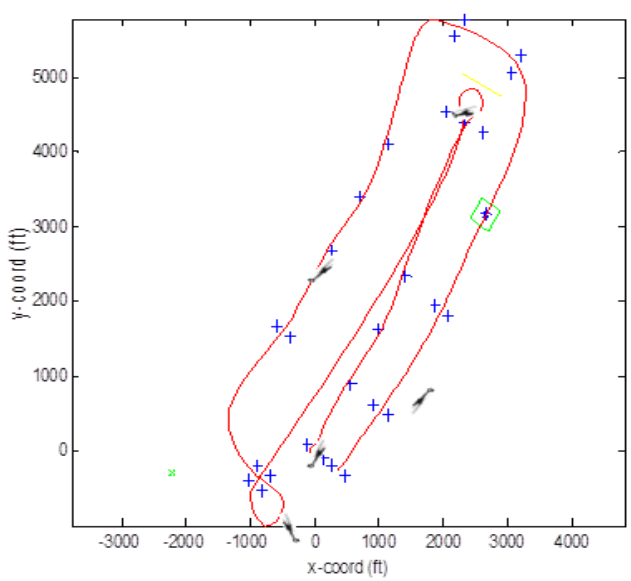

Figure 74. Optimal Trajetory

13 SURVIVABILITY & SAFETY

13.1 Minimum Equipment

Figure 75. Switlik ISPLR

Both RFP and FAA requirements mandate flotation for the pilot as well as fire protection as a minimum. The Switlik Inflatable Single Place Life Raft (ISPLR) is a small, lightweight military design flotation device, shown in Figure 75. The ISPLR is contained in a 7"x12" valise pack weighing a mere 5.4 pounds. It can easily be clipped to the pilot's flight suit ensuring access to it in the event of an ejection upon landing. It contains two 75 gram air cylinders which will quickly and automatically inflate the raft, allowing the pilot to safely float until emergency vehicles arrive.

The cockpit will also be stocked with a small, lightweight fire-extinguisher, similar to the model shown in Figure 76. Its compact, grenade-shape design will allow it to be stored somewhere out of the pilot's way, while still remaining easily accessible.

As for the pilot's seat, in order to obtain maximum safety and comfort while minimizing weight, a design was chosen from the BAE Systems S7000 line of crashworthy helicopter seats. One such model, shown in Figure 77, weighs as little as 56 pounds, while meeting both MIL-STD-58095A and MIL-STD-810 requirements. It contains a 5-point harness, inertia reel lock, vertical and horizontal adjustment, and bolstered cushioning. Other forms of Equipment required for the VFR Corridor of the Hudson River are listed below.

Table 27: Required Equipment

BADGER EQUIPMENT
Temperature Gauges
Engine Tachometer
Engine Pressure Gauge
Oil Pressure Gauge
Altimeter
Airspeed Indicator
Direction Indicator
Fuel Gauge
Safety Belt

Figure 77. BAE S7000 Seat

Figure 76. Fire Extinguisher

13.2 Autorotation

The autorotative index is a factor of stored kinetic energy in the rotor. It is a ratio of the rotor's kinetic energy ($I_R\Omega^2/2$) to the gross weight (W), normalized by disk loading according to the Sikorsky equation found in Leishman's *Principles of Helicopter Aerodynamics*. We know from empirical observations that a single engine helicopter should have an autorotative index value close to ~20. With a blade radius of 12.4ft, 670rpm, a weight of 2500lbs, and a disk loading of 2.59, the autorotative index for the Badger is calculated as 22.5, and its relation to other single engine helos can be seen here in Figure 78.

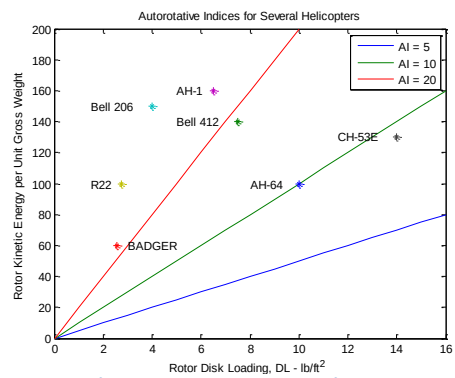

Figure 78. Autorotative Index

13.3 H-V Diagram

A helicopter's H-V diagram defines a region of operation which the pilot is encouraged to avoid in order to ensure a successful autorotation in the event of a power failure. The H-V curve also provides the pilot with a suggested trajectory to follow at takeoff when the helicopter is still low to the ground. It is typically drawn for a particular helicopter using a test procedure during certification. For the purposes of computing this curve during the preliminary design, Pegg (NASA TN D-4536) was used since it provides a semi-empirical method of computation. This diagram is shown in figure 79.

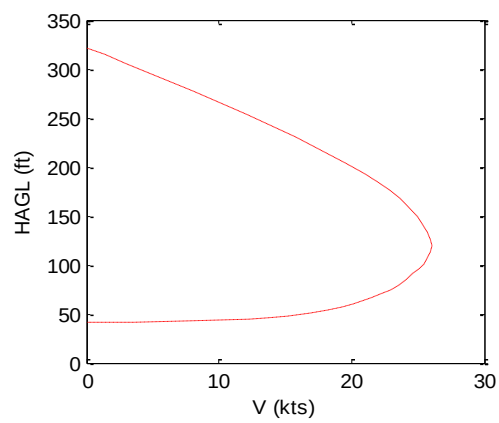

Figure 79. H-V Diagram

14 FEASIBILITY

14.1 Technology Readiness Level

Technology Readiness Levels (TRLs) were created by the DoD and NASA to assess the maturity of a certain technology. The effective use of TRLs can reduce the risk associated with investing in immature components. TRLs follow a scale from 1 (lowest level of readiness) to 9 (mature development). By the time a technology earns the TRL of 9, it has been deemed "flight qualified" and "flight proven".

The Badger only uses mature technologies within its design. Individually, every aspect of the helicopter would receive a TRL of 9 since each system has been proven through successful mission operations. However, since this helicopter is a completely new design, the integration of the technologies between each other assigns the Badger with a TRL of 7.5. This is due to the fact that the AFRL considers a TRL of 7 to be an acceptable risk for starting the engineering and manufactory development phase (Graettinger). The rotorcraft must therefore demonstrate the actual system prototypes in an operational environment to receive a higher rating. The expected date of the first built helicopter is in 2017.

14.1 Life-Cycle Cost Analysis

Table 28: Breakdown of Development Cost

System	Estimated Cost
Engineering	
Design	$24,410,000
Flight Test	$3,251,000
Component Test	$10,387,000
Systems Engineering/Project Management	$3,173,000
Manufacturing Engineering	
Planning, Loft, Other	$7,315,000
Project Management	$611,000
Tooling	
Tool make	$9,245,000
Outside Tooling	$5,403,000
Manufacturing	
Prototype	$2,496,000
No GTV, STA, or FTA Required	$0
Flight Test	$2,197,000
Component Test	$8,790,000
Logistics	$224,000
Other	
Travel and Per Diem	$941,000
Direct Expense	$4,838,000
Total Program	**$83,281,000**

The Bell PC Based Cost Model was used to calculate the total development cost and also to estimate the prototype and full production costs of The Badger. The total development cost of came out to be $83,281,000. Around 50% of the cost was attributed to engineering costs ($41,221,000), this is because it was developed as an entirely new system.

The cost for the first prototype was estimated to be around $3,000,000 with The Badger costing about $1,689,000 when in full production. This compares with the Kaman K-Max, an aircraft with a similar style configuration, which is estimated to cost $5,100,000 in full production.

15 FINAL SCORE AND SUMMARY

The scoring function given by the RFP is a combination of time, fuel weight, and engine power. The equation is:

$$\eta = 2 * course\ time\ [sec] + 5 * fuel\ consumed[lbs] + MRP_{S.L,\ ISA,\ Uninstalled}\ [SHP]$$

The Georgia Institute of Technology and the Middle East Technical University Badger Team have created an intermeshing helicopter that accomplishes a final score of:

$$\eta = 2 * 247.8s + 5 * 67lbs + 550\ SHP$$

$$\eta = 1380.6$$

The RFP required a more maneuverable rotorcraft than arguably any rotorcraft made before. This proposal presented the conceptual, preliminary, and final design process of an extremely unique rotorcraft. The stereotypical intermeshing rotor is considered to be a sluggish heavy lifter. It has been endearingly nicknamed an "air mule." While this is a fair statement for most current intermeshing rotorcraft, The Badger breaks this stereotype. It has high maneuverability while maintaining a minimal weight and power making it capable of completing the course efficiently and quickly. Previous intermeshing designs such as the Kaman K-Max were designed to be heavy lifters and thus defined the stereotype. However, through several iterations of the design process focusing on maneuverability, this configuration has become an effective racer. While certain helicopters may be better performers in some aspects than others, this is only due to the fact that they were designed to perform in that manner. Because the Badger was designed with maneuverability in mind, it is an effective racing rotorcraft. Not only does the Badger meet the criteria stated, but it also successfully outperforms the competition.

1
2
3

16 DETAILED WEIGHT BREAKDOWN

MIL- STD-1374 PART I - TAB PAGE 1

NAME GT MODEL BADGER

DATE 5/30/2012 REPORT

GROUP WEIGHT STATEMENT

AIRCRAFT

(INCLUDING ROTORCRAFT)

ESTIMATED - CALCULATED - ACTUAL

CONTRACT NO.	NA		
AIRCRAFT, GOVERNMENT NO.	NA		
AIRCRAFT, CONTRACTOR NO.	NA		
MANUFACTURED BY	BADGER CO.		
		MAIN	AUX
ENGINE QUANTITY	1		
ENGINE MANUFACTURED BY	NA		
ENGINE MODEL	NA		
ENGINE TYPE	NA		
PROPELLER QUANTITY	1		
PROPELLER MANUFACTURED BY	BADGER CO.		
PROPELLER MODEL	NA		
PAGES REMOVED	NONE	PAGE NO.	

Georgia Tech Rotorcraft Center of Excelence

MIL- STD-1374 PART I - TAB | GROUP WEIGHT STATEMENT (LBS) | PAGE 2

NAME GT | WEIGHT EMPTY | MODEL BADGER

DATE 5/30/2012 | REPORT

1	WING GROUP			WINGLETS	GLOVE / LEX	WING	
2	TOTAL						10
3	BASIC STRUCTURE						
4	CENTER SECTION						
5	INTERMEDIATE PANEL						
6	OUTER PANEL						
7	SECONDARY STRUCTURE						
8	AILERONS / ELEVONS						
9	SPOILERS						
10	FLAPS - TRAILING EDGE						
11	FLAPS - LEADING EDGE						
12	SLATS						
13							
14							
15	ROTOR GROUP						176
16	BLADE ASSEMBLY					76	
17	HUB AND HINGE					100	
18							
19	EMPENNAGE GROUP	CANARD	H. STAB.	VERT. FIN	VENT. FIN	TAIL ROTOR	
20	TOTAL		4	2			6
21	BASIC STRUCTURE						
22	SECONDARY STRUCTURE						
23	CONTROL SURFACES						
24	(INCL. BALANCE WEIGHTS)						
25	BLADES						
26	HUB AND HINGE						
27	ROTOR / FAN DUCT						
28							
29							
30	FUSELAGE GROUP				FUS./ HULL	BOOMS	
31	TOTAL						165
32	BASIC STRUCTURE						
33	SECONDARY STRUCTURE						
34	ENCLOSURES, FLORING, ETC.						
35	DOORS, RAMPS, PANELS						
36							
37							
38	ALIGHTING GEAR GROUP	MAIN	NOSE /TAIL		ARR. GEAR	CAT. GEAR	
39	TOTAL	35	9				44
40	RUNNING GEAR / FLOATS/ SKIS						
41	STRUCTURE						
42	CONTROLS						
43							
44							
45	ENGINE SECTION OR NACELLE GROUP	AUXILARY ENGINES		MAIN ENGINES			
46	LOCATION						
47	TOTAL - EACH LOCATIOIN						20
48							
49							
50	AIR INDUCTION GROUP	AUXILARY ENGINES		MAIN ENGINES			
51	LOCATION						
52	TOTAL - EACH LOCATION						1.5
53	INLETS						
54	DUCTS, ETC.						
55	TOTAL STRUCTURE						422.5

56	PROPULSION GROUP		AUX		MAIN		848
57	ENGINE					141	
58	ENGINE INSTALLATION					55	
59	ACCESSORY GEAR BOXES & DRIVE					55	
60	EXHAUST SYSTEM					55	
61	ENGINE COOLING				47		
62	WATER INJECTION				50		
63	ENGINE CONTROLS						
64	STARTING SYSTEM				15		
65	PROPELLER / FAN INSTALLATION					25	
66	LUBRICATING SYSTEM						
67	FUEL SYSTEM					55	
68	TANKS - PROTECTED				45		
69	TANKS - UNPROTECTED						
70	PLUMBING, TEC.				10		
71							
72	DRIVE SYSTEM					350	
73	GEAR BOXES, LUB SYS & RTR BRK				150		
74	TRANSMISSION DRIVE						
75	ROTOR SHAFTS				200		
76	GAS DRIVE						
77							
78	FLIGHT CONTROLS GROUP						
79	COCKPIT CONTROLS				100		
80	AUTOMATIC FLIGHT CONTROL SYSTEM						
81	SYSTEM CONTROLS						
82	AUXILIARY POWER GROUP						
83	INSTRUMENTS GROUP						25
84	HYDRAULIC GROUP						
85	PNEUMATIC GROUP						
86	ELECTRICAL GROUP					25	
87	AVIONICS GROUP					150	
88	EQUIPMENT				125		
89	INSTALLATION				25		
90	ARMAMENT GROUP						
91	FUNISHINGS & EQUIPMENT GROUP						
92	ACCOMODATION FOR PERSONNEL					185	
93	MISCELLANEOUS EQUIPMENT				100		
94	FURNISHINGGS				35		
95	EMERGENCY EQUIPMENT				200		
96	AIR CONDITIONING GROUP						
97	ANTI-ICING GROUP						
98	PHOTOGRAHIC GROUP						
99	LOAD & HANDLING GROUP					185	
100	AIRCRAFT HANDLING				85		
101	LOAD HANDLING				100		
102							
103	TOTAL SYSTEMS AND EQUIPMENT						
104	BALLAST GROUP						
105	MANUFACTURING VARIATION						150
106	CONTINGENCY						
107							
108	TOTAL CONTRACTOR CONTROLLED						
109	TOTAL CONTRACTOR - RESPONSIBLE						
110	TOTAL WEIGHT EMPTY PG. 2-3						1927

Georgia Tech Rotorcraft Center of Excelence

111	LOAD CONDITION						PRIMARY
112							
113	WEIGHT EMPTY						1927
114	CREW (empty)						
115	UNUSABLE FUEL					127	
116	OIL				50		
117	TRAPPED			10			
118	ENGINE			30			
119	TRANSMISSION DRIVE			10			
120	AUX. FUEL TANKS						
121	INTERNAL						
122	EXTERNAL						
123							
124	WATER INJECTION FLUID						
125	BAGGAGE						
126	GUN INSTALLATIONS						
127	GUNS						
128							
129							
130	SUPPORTS						
131	WEAPONS PROVISIONS						
132							
133	OTHER					200	
134							
135	CHAFF						
136	FLARES						
137							
138							
139	SURVIVAL KITS					20	
140	LIFE RAFTS					15	
141	OXYGEN					4	
142							
143							
144							
145	OPERATIONG WEIGHT					225	
146	PASSENGERS						
147							
148	CARGO				300		
149							
150	AMUNITION						
151							
152	WEAPONS						
153							
154							
155							
156							
157							
158	ZERO FUEL WEIGHT						
159	USABLE FUEL						
160	INTERNAL						
161							
162	EXTERNAL						
163							
164	TOTAL USEFUL LOAD						
165	GROSS WEIGHT						2792

Georgia Tech Rotorcraft Center of Excelence

17 REFERENCES

1 Johnson, W. (1994). Helicopter theory. New York: Dover Publications.

2 Leishman, J. Gordon. (2000). Principles of helicopter aerodynamics. Cambridge: Cambridge University Press.

3 Engineering Design Handbook: Helicopter Engineering. Part One *Preliminary Design*. Vol. AMCP 706-201. Washington, D.C.: Headquarters, U.S. Army Materiel Command, 1972. Print.

4 Abbott, Ira H. A., and Albert Edward Von Doenhoff. *Theory of Wing Sections; including a Summary of Airfoil Data,*. New York: McGraw-Hill, 1949. 462. Print.

5 Schrage, Daniel P. "GIT-KKU IPPD Rotorcraft Preliminary Design Methodology." (2009). Print.

6 Drees, Jan M., Larry W. Dooley, and Willliam D. Neathery. Compound Hub Spring System for Helicopters. Textron, Inc., assignee. Patent 4333728. 8 June 1982. Print.

7 Singh, Kiran. "Servo Flap Controlled Rotor." *Servo Flap Controlled Rotor*. Helicopter History Site. Web. 16 Feb. 2012. <http://www.helis.com/howflies/servo.php>.

8 Tishchenko, M.,N., V. T. Nagaraj, and I. Chopra. Unmanned transport helicopter. In 55th Annual Forum Proceedings. American Helicopter Society, Montreal, Canada, May 1999.

9 Graettinger, Caroline P. "Using the Technology Readiness Levels Scale to Support Technology Management in the DoD's ATD/STO Environments." *CMU/SEI-2002-SR-027* (2002). Print.

10 "JavaProp" Willkommen / Welcome. Web. 28 Mar. 2012. <http://www.mh-aerotools.de/>.

11 Federal Aviation Administration <http://www.faa.gov>

12 Tishchenko, M. N., Nagaraj, V. T., and Chopra, I., "Preliminary Design of Transport Helicopters,"

13 Journal of the American Helicopter Society, Vol. 48, No. 2, April 2003, pp. 71–79.

14 J. W. Rutherford and S. M. Bass. The design evolution of the canard rotor/wing. In AHS 49th Annual Forum Proceedings. American Helicopter Society, May 1993.

15 1999. Website: http://amber.aae.uiuc.edu/ m-selig/ads/coord database.html, UIUC Airfoil Coordinates and Performance Database, 1999.

16 P. D. Talbot. High speed rotorcraft: Comparison of leading concepts and technology needs. In 47th Annual Forum Proceedings. American Helicopter Society, Phoenix, AZ 1991.

17 L. Young, D. Grahm, and R. Straub. Reduction of hub- and pylon-fairing drag. In 43rd AnnualForum Proceedings, pages 323{344. American Helicopter Society, St. Louis, Missouri, May 1987.

18 Prouty R. Rotary-Wing Performance, Stability and Control. Robert E. Krieger Publishing Company, Malabar, FL, 1990.

19 C.W. Nelson. Airplane Propel ler Principles. John Wiley & Sons, Inc., Ames, IA, 1944.

20 J. Kish. Sikorsky aircraft advanced rotorcraft transmission (ART) program- nal report. NASA Contractor Report CR-191079, NASA, March 1993

21 Dowty. Advanced Technology Propel lers. Dowty Aerospace Propellers, Gloucester, England, 1997. Issue 5.

22 D. Biermann and E. P. Hartman. Wind-tunnel tests of four and six blade single- and dual-rotating propellers. NACA Report 747, NACA, 1940.

23 N. S. Currey. Aircraft Landing Gear Design : Principles and Practices. American Institute of Aeronautics and Astronautics, Washington, D.C., 1988.

24 D. Dudley. Handbook of Practical Gear Design. McGraw-Hill Cook Company, New York, 1984.